AMERICAN SOCIETY FOR MICROBIOLOGY | Infection and Immunity®

MOLECULAR PATHOGENESIS

# Role of *metAB* in Methionine Metabolism and Optimal Chicken Colonization in *Campylobacter jejuni*

**Brandon Ruddell,[a] Alan Hassall,[a,b] Orhan Sahin,[b] Qijing Zhang,[a] Paul J. Plummer,[a,b] Amanda J. Kreuder[a,b]**

[a]Department of Veterinary Microbiology and Preventive Medicine, College of Veterinary Medicine, Iowa State University, Ames, Iowa, USA
[b]Department of Veterinary Diagnostic and Production Animal Medicine, College of Veterinary Medicine, Iowa State University, Ames, Iowa, USA

**ABSTRACT** *Campylobacter jejuni* is a zoonotic pathogen and is one of the leading causes of human gastroenteritis worldwide. *C. jejuni* IA3902 (representative of the sheep abortion clone) is genetically similar to *C. jejuni* W7 (representative of strain type NCTC 11168); however, there are significant differences in the ability of *luxS* mutants of these strains to colonize chickens. LuxS is essential for the activated methyl cycle and generates homocysteine for conversion to L-methionine. Comparative genomics identified differential distribution of the genes *metA* and *metB*, which function to convert homoserine for downstream production of L-methionine, between IA3902 and W7, which could enable a secondary pathway for L-methionine biosynthesis in a W7 Δ*luxS* but not in an IA3902 Δ*luxS* strain. To test the hypothesis that the genes *metA* and *metB* contribute to L-methionine production and chicken colonization by *Campylobacter*, we constructed two mutants for phenotypic comparison, the W7 Δ*metAB* Δ*luxS* and IA3902 Δ*luxS*::*metAB* mutants. Quantitative reverse transcription-PCR and tandem mass spectrometry protein analysis were used to validate MetAB transcription and translation as present in the IA3902 Δ*luxS*::*metAB* mutant and absent in the W7 Δ*metAB* Δ*luxS* mutant. Time-resolved fluorescence resonance energy transfer fluorescence assays demonstrated that L-methionine and *S*-adenosyl methionine concentrations decreased in the W7 Δ*metAB* Δ*luxS* mutant and increased in the IA3902 Δ*luxS*::*metAB* mutant. Assessment of chicken colonization revealed that the IA3902 Δ*luxS*::*metAB* strain partially rescued the colonization defect of the IA3902 Δ*luxS* strain, while the W7 Δ*metAB* Δ*luxS* strain showed significantly decreased colonization compared to that of the wild-type and the W7 Δ*luxS* strain. These results indicate that the ability to maintain L-methionine production *in vivo*, conferred by *metA* and *metB* in the absence of *luxS*, is critical for normal chicken colonization by *C. jejuni*.

**KEYWORDS** *Campylobacter jejuni*, central metabolism, colonization, methionine

*Campylobacter jejuni* is one of the leading causes of human gastroenteritis worldwide (1). As a zoonotic pathogen, transmission has been linked to ruminant contact (1), raw chicken meat (2, 3), consumption of raw milk (4), and environmental exposure from contaminated water supplies (5, 6). In the United States, the *Campylobacter jejuni* sheep abortion (SA) clone (represented by isolate IA3902) has recently emerged as the dominant pathogen causing ovine abortions, and SA clone-associated human outbreaks have been reported (7, 8). While the SA clone displays significant genetic similarity to the commonly studied NCTC 11168 strain (9–12), both strains demonstrate distinct colonization phenotypes after disrupting enzyme *S*-ribosylhomocysteine lyase (LuxS), despite 100% gene homology between these strains. (10, 12). In IA3902, *luxS* mutants have been demonstrated to display disrupted *in vivo* colonization using the chicken colonization model (10, 13). However, inactivation of *luxS* in W7, a highly motile variant of NCTC 11168, does not disrupt colonization of the chicken ceca (10).

LuxS is a critical enzyme within the activated methyl cycle (AMC); the AMC serves an

**Citation** Ruddell B, Hassall A, Sahin O, Zhang Q, Plummer PJ, Kreuder AJ. 2021. Role of *metAB* in methionine metabolism and optimal chicken colonization in *Campylobacter jejuni*. Infect Immun 89:e00542-20. https://doi.org/10.1128/IAI.00542-20.

**Editor** Guy H. Palmer, Washington State University



Address correspondence to Amanda J. Kreuder, akreuder@iastate.edu.

**Received** 28 August 2020
**Returned for modification** 8 September 2020
**Accepted** 4 October 2020
**Accepted manuscript posted online** 12 October 2020
**Published** 15 December 2020

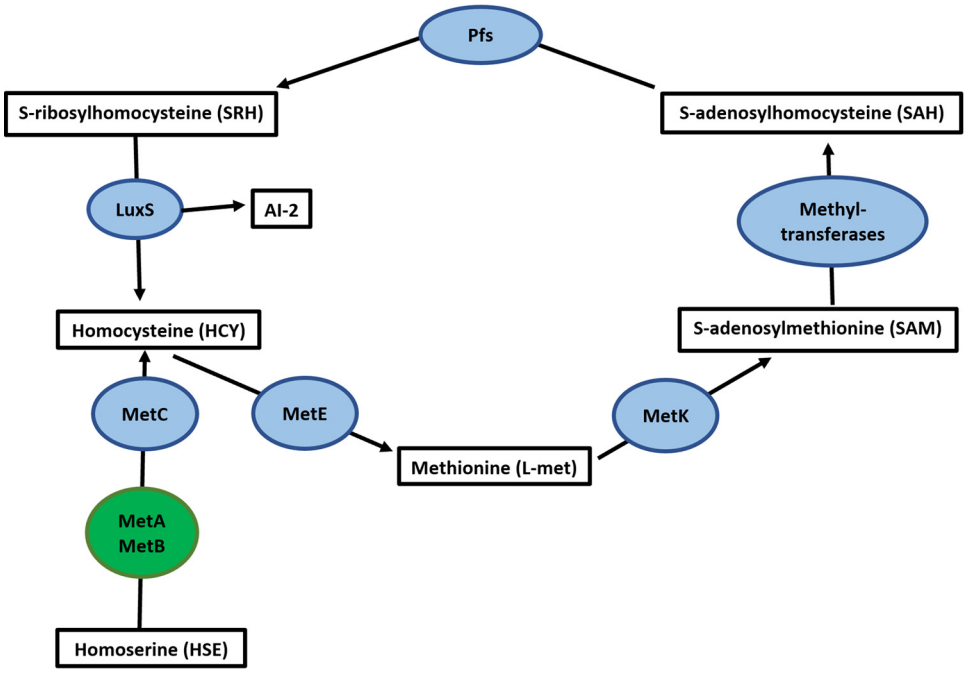


**FIG 1** Known *C. jejuni* enzymes and metabolic products of the activated methyl cycle (AMC) involved in the production of AI-2, methionine, and SAM. Boxes indicate metabolic products of enzymes within the AMC. Circles indicate the following enzymes utilized in the AMC: LuxS, S-ribosylhomocysteine lyase; MetE, methionine synthase; MetK, SAM synthase; methyl transferases; Pfs, *S*-adenosylhomocysteine nucleosidase; MetA, homoserine O-succinyltransferase; MetB, O-succinylhomoserine (thiol) lyase; MetC, cystathionine lyase. Green circles indicate additional enzymes encoded by *C. jejuni* W7 that are not found in *C. jejuni* IA3902. LuxS produces two byproducts, AI-2 and homocysteine. MetK produces SAM, which enables the transfer of methyl groups (-$CH_3$) to various substances and SAM-dependent reactions. SAH is toxic and must be recycled by Pfs.

essential role in bacterial central metabolism, including downstream production of important metabolic products such as L-methionine (L-met) and *S*-adenosylmethionine (SAM) (Fig. 1) (14). Within the AMC, the enzyme LuxS produces homocysteine, which is then used directly for L-met production; the availability of L-met is critical for downstream production of SAM (14). During the production of homocysteine, LuxS also produces 4,5-dihydroxy-2,3-pentanedione (DPD), which cyclizes to form a mixture of furanones that includes autoinducer-2 (AI-2) derivatives (15). AI-2 is a quorum sensing molecule that has been demonstrated in many species of bacteria to be critical for gene regulation, influencing many phenotypes, including motility, biofilm formation, susceptibility to antibiotics, virulence factor modulation, and others (14, 16, 17). While the exact role of AI-2 in *Campylobacter* spp. remains debatable (16, 18), the dual function of LuxS and its interconnection with the AMC complicates the ability to determine which enzymatic byproducts are most responsible for phenotypic changes that are observed with the loss of LuxS in *C. jejuni*. As genetic complementation of *C. jejuni luxS* mutants alone does not enable investigators to discern the unique roles that AMC metabolic byproducts or AI-2 utilization may play in the phenotypic defects observed, alternative approaches to studying each function independently are necessary (10). AI-2 production is equally lost in both W7 and IA3902 with the loss of LuxS; therefore, the observed difference in colonization between these two strains provides a unique opportunity to further investigate the role of the AMC and L-methionine metabolism in the pathophysiology of *C. jejuni*.

While L-met biosynthesis and AMC pathways have been well studied in model organisms such as *Escherichia coli* and *Salmonella*, there is currently a paucity of information in this area concerning *C. jejuni* (14, 19, 20). However, genetic comparisons using the well-characterized *E. coli* model can enable a prediction of the AMC pathway in *C. jejuni* (Fig. 1). Interestingly, while the core AMC pathway remains similar between

**TABLE 1** Methionine biosynthesis pathways

| Pathway or component | *E. coli* | *C. jejuni* W7[a] | *C. jejuni* IA3902[a] |
|---|---|---|---|
| Acetylation | | | |
| Substrate | Homoserine | Homoserine | —[c] |
| Enzyme | MetA | MetA[b] | — |
| Product | O-succinylhomoserine | O-succinylhomoserine | — |
| Trans-sulfurylation (step 1) | | | |
| Substrate | O-succinylhomoserine | O-succinylhomoserine | — |
| Enzyme | MetB | MetB[b] | — |
| Product | Cystathionine | Cystathionine | — |
| Trans-sulfurylation (step 2) | | | |
| Substrate | Cystathionine | Cystathionine | Cystathionine |
| Enzyme | MetC | MetC | MetC |
| Product | Homocysteine | Homocysteine | Homocysteine |
| Activated methyl cycle (AMC) | | | |
| Substrate | *S*-ribosyhomocysteine | *S*-ribosyhomocysteine | *S*-ribosyhomocysteine |
| Enzyme | LuxS | LuxS | LuxS |
| Product | Homocysteine and AI-2 | Homocysteine and AI-2 | Homocysteine and AI-2 |
| Methylation of homocysteine | | | |
| Substrate | Homocysteine | Homocysteine | Homocysteine |
| Enzyme | MetH/MetE | —/MetE | —/MetE |
| Product | L-Methionine (L-met) | L-Methionine (L-met) | L-Methionine (L-met) |

[a]*Campylobacter jejuni* strains.
[b]*C. jejuni* W7 MetAB, 100% coverage versus *E. coli* MG165 K-12.
[c]—, Not encoded in the genome.

strains IA3902 and W7, there is divergence between these strains regarding the presence of a redundant system for production of L-met (12). In addition to LuxS, which produces homocysteine for conversion to L-met and is present in all *C. jejuni* strains, W7 encodes a separate pathway for homocysteine production used for downstream methionine production via the *metA* and *metB* genes that are not encoded on the genome of IA3902 (12) (Table 1). Beginning with substrate homoserine, the enzymes homoserine O-succinyltransferase (MetA) and O-succinylhomoserine (thiol)-lyase (MetB) act to produce cystathionine, which can then be acted upon by the enzyme cystathionine beta-lyase (MetC) to form homocysteine; MetC is present in both W7 and IA3902.

Based on this observation, we hypothesized that deletion of *luxS* in IA3902 disrupts *de novo* synthesis of L-met and downstream production of SAM and other AMC pathway determinants, specifically under methionine-depleted conditions such as those encountered in the gastrointestinal tract when transport alone cannot provide for all needs, leading to failure to colonize. However, LuxS-deficient W7 can produce L-met using the alternative MetA and MetB system, feeding L-met into the AMC and resulting in no phenotypic defect in *in vivo* colonization. To test this hypothesis, we created a W7 Δ*metAB* Δ*luxS* mutant to disrupt L-met biosynthesis in W7 to mimic the IA3902 Δ*luxS* strain, and an IA3902 Δ*luxS*::*metAB* mutant to introduce the secondary L-met biosynthesis route found in the W7 Δ*luxS* strain. Using quantitative reverse transcriptase PCR (qRT-PCR) and proteomics, we were able to demonstrate altered MetAB expression in our mutant constructs. Next, we observed that the addition of *metAB* increases L-met and SAM production in the IA3902 Δ*luxS* strain *in vitro*, while the deletion of *metAB* from the W7 Δ*luxS* strain decreases *in vitro* L-met and SAM levels. Finally, utilizing the chicken colonization model, we demonstrated that the addition of *metAB* to the IA3902 Δ*luxS* strain leads to partial rescue of the defect observed in chicken colonization by the IA3902 Δ*luxS* strain, while deletion of *metAB* from the W7 Δ*luxS* strain leads to reduced chicken colonization. These results indicate that L-met production is critical for optimal chicken cecum colonization by *C. jejuni* and warrants further studies on the role of central methionine metabolism in the pathogenicity of this zoonotic pathogen.

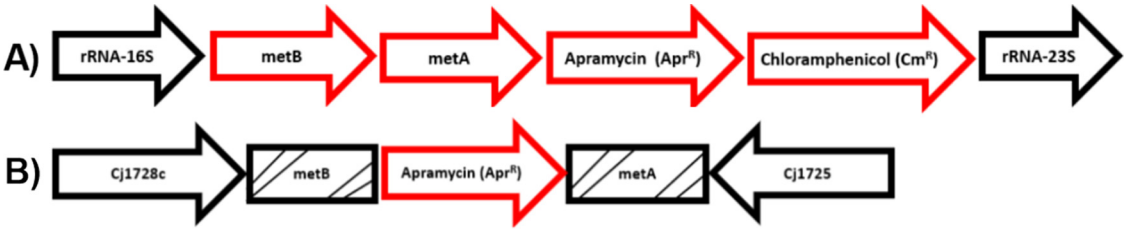


**FIG 2** Mutant constructs of *Campylobacter jejuni* IA3902 Δ*luxS*::*metAB* and W7 Δ*luxS* Δ*metAB* strains, corresponding to the depicted genome. (A) Operon *metAB* insertion within the IA3902 Δ*luxS* strain. (B) Operon *metAB* insertional deletion within the W7 Δ*luxS* strain. Red arrows indicate genomic insertions via homologous recombination. Boxes with a strikethrough indicate gene-specific insertional deletions.

## RESULTS

**Identification of the *metAB* operon within NCTC 11168 and mutant generation.** BLASTN sequence analysis of the *metA* and *metB* genes encoded by NCTC 11168 revealed that more than 100 *C. jejuni* strains encode both genes, with high conservation across the species and both notably absent in IA3902. Within *C. jejuni* NCTC 11168, the *metA* and *metB* genes are located at nucleotide positions 1635432 to 1637686 (Cj1726c and Cj1727c) within hypervariable region 12 (12); interestingly, no other known AMC pathway genes are found near this location. Further analysis of this location via BLASTN sequence analysis revealed a single promoter region for *metB* and minimal intergenic space between *metB* and downstream *metA*, suggestive of an operon structure. Additionally, Operon-mapper (21) predicted a single operonic gene pair with 95% probability when analyzing genes *metA* and *metB*.

Therefore, to begin to study the role of redundant L-met biosynthesis in *luxS*-deficient mutants of *C. jejuni*, the *metAB* operon was first inserted into the intergenic region between the 16S and 23S rRNA operon (rrs-rrl) of the IA3902 Δ*luxS* strain (10) via homologous recombination to create the IA3902 Δ*luxS*::*metAB* mutant (Fig. 2). In parallel, the *metAB* operon was inactivated in the W7 Δ*luxS* strain (10) via the insertion of an apramycin resistance cassette via homologous recombination, creating the W7 Δ*luxS* Δ*metAB* mutant (Fig. 2). Successful mutant constructs were confirmed via Sanger sequencing prior to further use.

**Normal growth in nutrient-rich medium and unaltered motility of *metAB* mutant constructs compared to that of the parent *luxS*-deficient strain.** To determine the effect of alteration of *metAB* in *luxS*-deficient mutants on growth, *in vitro* growth curves were performed in triplicate using Mueller-Hinton (MH) broth. The growth over a period of 30 h was analyzed by collecting optical density readings ($A_{600}$) and CFU/ml counts; Fig. 3A and B demonstrate that the growth of mutant strains is normal relative to that of wild-type strains. Based on analysis of CFU/ml counts, all strains reached the early stationary phase of growth by 12 h. There was no statistically significant difference between strains using either the average optical density ($A_{600}$) or CFU/ml ($P > 0.05$) over 30 h via analysis using two-way analysis of variance (ANOVA); however, the W7 strains tended to grow at lower rates than the IA3902 strains. Therefore, for further comparative phenotype studies, samples were collected at staggered time points (12 h for IA3902 and 14 h for W7 strains) for similar average $A_{600}$ and CFU/ml values, at the early stationary phase of growth. Further analysis via one-way ANOVA revealed no statistical difference in average $A_{600}$ or CFU/ml at the staggered time point collection when comparing all strains (Fig. 3C and D).

Motility assays in semisolid agar were performed not only to confirm that the introduced mutations did not inadvertently lead to a lack of motility, as motility is a key colonization and virulence attribute of *Campylobacter* that enables colonization of the intestinal mucosal lining (22, 23), but also to evaluate the effect of multiple L-met biosynthesis pathways on motility *in vitro*. Figure 4 demonstrates the results and confirms that all the strains were able to grow and remain motile on motility agar over 30 h. Significant phenotypic differences ($P < 0.05$) between wild-type strains and mu-

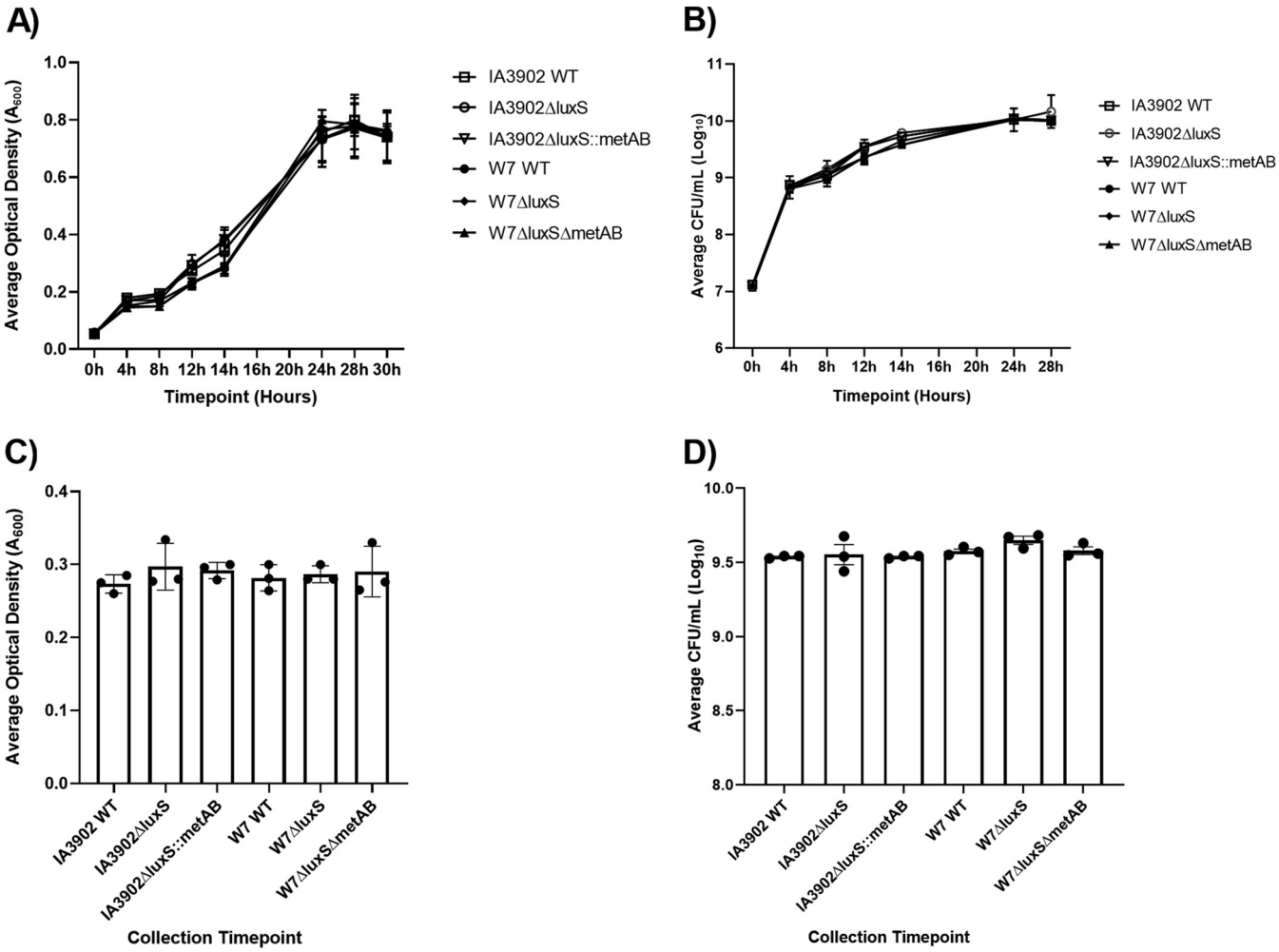


**FIG 3** Shaking growth curve of the IA3902 wild type (WT), W7 WT, and isogenic mutants reveal that growth is normal (mean ± standard error of the mean [SEM]). Results of three biological replicates of shaking growth curves performed in 250-ml Erlenmeyer flasks under microaerophilic conditions in standard Mueller-Hinton (MH) broth. (A) Growth curve expressed as optical density ($A_{600}$) over time. (B) Growth curve expressed as CFU/ml over time. (C) Growth curve average expressed as optical density ($A_{600}$) at the collection time point (12 h for IA3902 and 14 h for W7 strains; early stationary phase). (D) Growth curve average expressed as CFU/ml at the collection time point (12 h for IA3902 and 14 h for W7 strains; early stationary phase). Analysis via two-way analysis of variance (ANOVA) revealed no significant difference among the growth curves of strains (A and B) ($P > 0.05$). One-way ANOVA of the growth curve averages at the defined collection time points (C and D) demonstrated no significant difference ($P > 0.05$).

tants were identified. The IA3902 Δ*luxS* and W7 Δ*luxS* strains had significantly decreased average motility ($P < 0.05$) compared to that of their respective wild-type strains, as previously reported (10, 13), with both new IA3902 Δ*luxS*::*metAB* and W7 Δ*luxS* Δ*metAB* mutant constructs also exhibiting a statistically significant decreased motility compared to that of both wild-type strains ($P < 0.05$). However, altered L-met biosynthesis via insertion or deletion of *metAB* did not significantly influence motility compared to that of the parent *luxS*-deficient strains ($P > 0.05$). There was a slight increase in motility of the IA3902 Δ*luxS*::*metAB* strain compared to that of the IA3902 Δ*luxS* parent strain; however, significance was not detected ($P > 0.05$). The data confirm previous studies which have demonstrated that mutation of *luxS* hinders motility, but indicate for the first time that the presence or absence of the *metA* and *metB* genes does not appear to significantly contribute to motility *in vitro*.

***metA* and *metB* are transcribed and translated in the IA3902 Δ*luxS*::*metAB* strain but not in the W7 Δ*luxS* Δ*metAB* strain.** qRT-PCR and proteomics via liquid chromatography with tandem mass spectrometry (LC-MS/MS) were next utilized to analyze *metAB* transcription and translation in the IA3902 Δ*luxS*::*metAB* and W7 Δ*luxS* Δ*metAB* strains. Transcription of *metAB* was significantly increased ($P < 0.05$) when

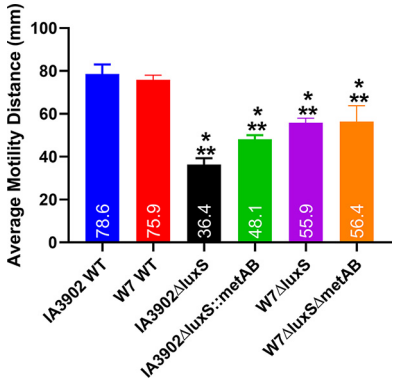


**FIG 4** Motility assays confirm that isogenic mutants remain motile, and L-met biosynthesis does not influence motility *in vitro* (mean ± SEM). Respective wild-type (WT) strains and isogenic mutant strains were normalized to the same $A_{600}$ of 0.300 and inoculated on 0.4% motility soft agar medium, and the average distance of motility was measured at 30 h of incubation at 42°C under microaerobic conditions. Each bar represents the average motility of three biological replicates consisting of six technical replicates during each independent study. One-way ANOVA followed by Tukey's multiple-comparison analysis demonstrated significance ($P < 0.05$). All *luxS* background mutants had significantly decreased motility ($P < 0.05$) compared to that of both WT strains. L-Met biosynthesis via insertion or deletion of *metAB* did not influence motility significantly compared to that of *luxS*-deficient parent strains ($P > 0.05$). *, Significance compared to IA3902 WT; **, significance compared to W7 WT.

comparing the IA3902 Δ*luxS*::*metAB* strain to all other strains (see Fig. S1 in the supplemental material). The fold change in expression levels of *metAB* in the IA3902 Δ*luxS*::*metAB* strain increased by 13.31-fold (standard error of the mean [SEM], ±2.94) over that of the W7 wild type. Additionally, IA3902 wild-type and W7 Δ*luxS* Δ*metAB* strains had no *metAB* mRNA transcription detected beyond the threshold cycle ($C_T$) level cutoff 35, which indicated that *metAB* was not expressed in these strains. Thus, both W7 wild-type and IA3902 Δ*luxS*::*metAB* strains were confirmed to transcribe *metAB*, while IA3902 and W7 Δ*luxS* Δ*metAB* strains had no *metAB* transcription detected. Analysis of control 16S mRNA transcriptional levels revealed no statistical significance ($P > 0.05$) when comparing expression between strains, indicating that the overall transcriptional expression is otherwise similar between strains.

Next, proteomics were utilized to analyze translation of MetAB in IA3902 Δ*luxS*::*metAB* and W7 Δ*luxS* Δ*metAB*. First, SDS-PAGE was performed on whole-cell protein lysate harvested from early stationary-phase cultures. The results of the SDS-PAGE analysis demonstrated similar protein profiles between wild-type strains and the mutant constructs, confirming that these strains were harvested at a similar growth phase (see Fig. S2 in the supplemental material). However, as no visual differences were seen in the predicted region of MetA and MetB expression, whole-cell protein analysis was determined insufficient to detect differences in MetA and MetB translation. Therefore, gel slices were cut at the predicted MetA and MetB molecular sizes, 34.2 kDa and 46.7 kDa, respectively, for further quantitative proteomic analysis via LC-MS/MS using the IA3902 Δ*luxS*::*metAB* and W7 Δ*luxS* Δ*metAB* strains as representatives of positive and negative strains, respectively. Table 2 shows the results of the LC-MS/MS proteomic analysis, which demonstrates that MetAB proteins were present in the IA3902 Δ*luxS*::*metAB* strain and absent in the W7 Δ*luxS* Δ*metAB* strain, consistent with the qRT-PCR results of mRNA transcription (Fig. S1). Specifically, for the IA3902 Δ*luxS*::*metAB* strain, MetA had an average number of unique peptides detected of 2 (standard deviation [SD], ±0.0) and MetB had an average number of unique peptides of 23 (SD, ±0.71). MetA had an average number of peptide spectrum matches (PSMs) of 3.5 (SD, ± 0.71) with an average Mascot score of 185.5 (SD, ±55.9), and MetB had an average number of PSMs of 128.5 (SD, ±6.4) with an average Mascot score of 5758.5 (SD, ±376.9). These results demonstrated highly specific peptide matches to the protein of interest, with both proteins exhibiting high-confidence PSMs matching to the theoretical fragmentation patterns and Mascot scores above a 95% confidence rating. Together, these

**TABLE 2** Average protein identification information of isogenic mutants for proteins MetA and MetB

| Strain or protein | Protein | Avg no. of peptides[a] (±SD) | Avg no. of PSMs[b] (±SD) | Avg Mascot score[c] (±SD) | MW[d] (kDa) |
|---|---|---|---|---|---|
| IA3902 Δ*luxS*::*metAB* | | | | | |
| Homoserine O-succinyltransferase | MetA | 2 (0.0) | 3.5 (0.71) | 185.5 (55.9) | 34.2 |
| O-succinylhomoserine (thiol)-lyase | MetB | 23 (0.71) | 128.5 (6.4) | 5,758.5 (376.9) | 46.7 |
| W7 Δ*luxS* Δ*metAB* | | | | | |
| Homoserine O-succinyltransferase | MetA | ND[e] | ND | ND | ND |
| O-succinylhomoserine (thiol)-lyase | MetB | ND | ND | ND | ND |

[a]Average number of unique peptide sequences matching solely to the protein indicated.
[b]Average number of peptide spectrum matches (unique and redundant).
[c]Average sum of the scores of all PSMs; >95% confidence proteins are listed.
[d]MW, predicted molecular weight of protein of interest.
[e]ND, not detected (below detection threshold).

findings indicate that MetA and MetB were translated in the IA3902 Δ*luxS*::*metAB* strain but not in the W7 Δ*luxS* Δ*metAB* strain, further validating the mutant constructs.

**L-Met and SAM intracellular concentrations are increased by MetAB.** Previous work has demonstrated that IA3902 *luxS* mutants have altered AMC metabolites (24). To determine if MetAB directly alters L-met and downstream SAM biosynthesis within the AMC in *luxS*-deficient mutants, changes to intracellular L-met and SAM concentrations were measured using time-resolved fluorescence resonance energy transfer (TR-FRET) assays. As shown in Fig. 5, L-met concentration in the IA3902 Δ*luxS*::*metAB* strain was significantly increased ($P < 0.05$) compared to that in all other strains; in contrast, the average L-met concentration in the W7 Δ*luxS* Δ*metAB* strain was significantly reduced ($P < 0.05$) compared to that in all other strains. Both IA3902 Δ*luxS* and W7 Δ*luxS* strains showed reduced average L-met concentrations compared to those of their respective wild-type strains, but the difference was not statistically significant ($P > 0.05$).

Similarly, the IA3902 Δ*luxS*::*metAB* strain had significantly increased ($P < 0.05$) average SAM concentration compared to those of all other strains; in contrast, the W7 Δ*luxS* Δ*metAB* strain had a significant reduction ($P < 0.05$) in average SAM concentration compared to all other strains. Both the IA3902 Δ*luxS* and W7 Δ*luxS* strains had reduced average SAM concentrations compared to those of their respective wild-type parent

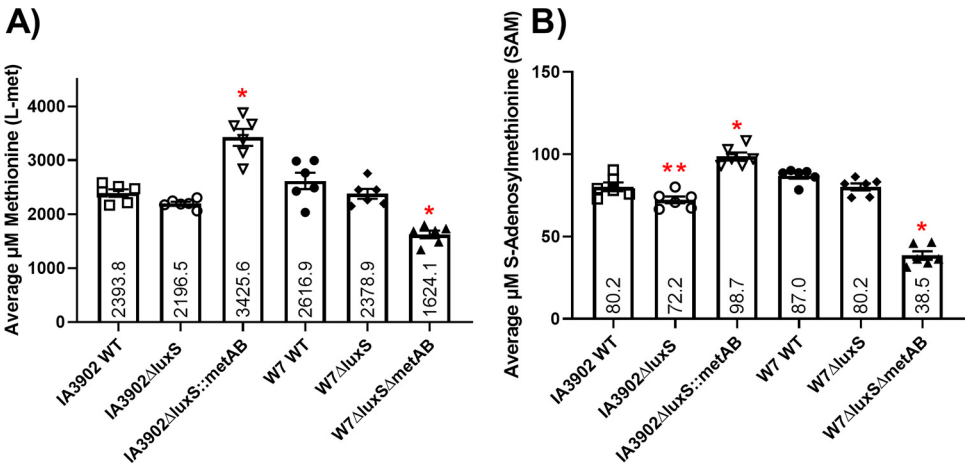


**FIG 5** The IA3902 Δ*luxS*::*metAB* mutant increases L-met and SAM concentrations, and the W7 Δ*luxS* Δ*metAB* mutant reduces L-met and SAM concentrations (mean ± SEM). (A) Time-resolved fluorescence resonance energy transfer (TR-FRET) assay results indicating intracellular L-methionine (L-met) extracted from bacterial cells at the early stationary phase of growth. (B) TR-FRET assay results indicating intracellular *S*-adenosylmethionine (SAM) extracted from bacterial cells at the early stationary phase of growth. Each bar represents the average metabolite concentration from three biological replicates. Metabolite concentration were calculated using a standard curve for each metabolite (L-met or SAM). For both panels A and B, independent one-way ANOVA with Tukey's multiple-comparison test demonstrated significance between strains ($P < 0.05$). For both panels A and B, significance versus all other strains is denoted by *, while significance ($P < 0.05$) versus the W7 wild-type (WT) only is denoted by **.

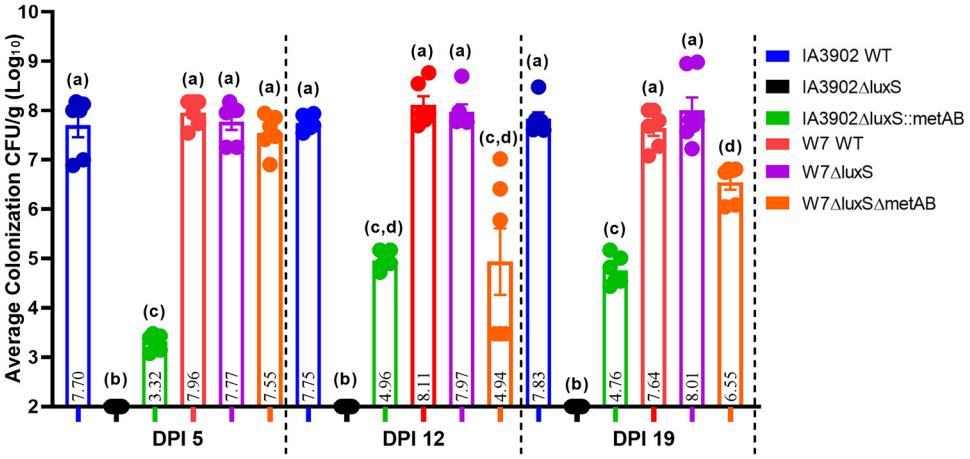


**FIG 6** Weekly chicken cecal colonization levels by wild-type (WT) strains and isogenic mutants at 5 dpi (week 1), 12 dpi (week 2), and 19 dpi (week 3) (geometric mean ± SEM). Each bird was orally inoculated with 200 $\mu$l of $5 \times 10^7$ CFU/ml bacterial suspension (approximately $1 \times 10^7$ CFU total per bird) using each respective strain. Each bar shows the average $\log_{10}$ CFU/g in the cecal contents in each group consisting of a minimum of 6 birds at each dpi point; results for individual birds are shown by circles within each bar. The limit of detection (LOD) was set at 100 CFU/g of cecal content. Significant differences ($P < 0.05$) in colonization were tested using one-way ANOVA at each dpi point with Tukey's multiple-comparison test to determine significance between biological groups. Significance between biological groups is indicated by lowercase letters. Overlap in letters indicates no significance ($P > 0.05$) at each dpi point.

strains, but the differences were not statistically significant ($P > 0.05$). These results indicate that the *metAB* operon contributes to the intracellular L-met and downstream SAM pool available for cellular usage *in vitro*.

***metAB* is required for optimal chicken colonization.** To determine if *metAB* contributes to *Campylobacter* colonization in the intestinal tract, a chicken colonization model as previously described (10, 13) was utilized to determine the colonization ability of mutants with altered methionine biosynthesis capabilities. Three-day-old chicks were orally inoculated with approximately $10^7$ CFU per strain of *C. jejuni*, followed by humane euthanasia of 6 chicks once weekly for 3 weeks to collect cecal contents for analysis of colonization levels via plating of serial dilutions and colony counts. As demonstrated in Fig. 6, the W7 Δ*luxS* strain maintained an ability to colonize chickens similar to W7 wild-type levels at each day postinoculation (dpi) time point, showing no statistical difference ($P > 0.05$). In contrast, IA3902 Δ*luxS* strain colonization abolishment to below the limit of detection was observed at each dpi point and was statistically different ($P < 0.05$) compared to that of the IA3902 wild type. With the insertion of the *metAB* genes, the IA3902 Δ*luxS*::*metAB* strain regained the ability to colonize chickens. The colonization level was significantly ($P < 0.05$) higher than that of the IA3902 Δ*luxS* parent strain at each dpi point but was still below the level of the IA3902 wild type, indicating that the complementary effect of *metAB* was partial. In contrast, the deletion of the *metAB* genes in the W7 Δ*luxS* Δ*metAB* strain significantly ($P < 0.05$) decreased its colonization level compared to that of the W7 Δ*luxS* parent strain at 12 and 19 dpi, but inactivation of *metAB* within the W7 Δ*luxS* background did not abolish its colonization ability. The observation that colonization patterns of the W7 Δ*luxS* Δ*metAB* strain did not match colonization patterns of complete abolishment seen in the IA3902 Δ*luxS* strain, nor did the IA3902 Δ*luxS*::*metAB* strain completely restore cecum colonization levels seen in the W7 Δ*luxS* and the wild-type strains, suggests that there are additional factors that contribute to colonization differences between these *C. jejuni* strains.

## DISCUSSION

The major conclusions of the current study demonstrate that redundancy of L-met biosynthesis via the presence of *metAB* in W7 but not IA3902 at least partially explains the differences in colonization ability previously observed between *luxS*-deficient mu-

tants of these strains. We also demonstrate that in the absence of LuxS, MetAB contributes to the intracellular L-met pool and downstream SAM production, two metabolites interconnected to the AMC found in *C. jejuni*. This experimental evidence strongly supports the notion that direct L-met utilization or utilization of L-met within the AMC are key contributing factors in the pathobiology of *Campylobacter jejuni*, as we clearly demonstrated that alteration of MetAB L-met production in *luxS*-deficient mutants directly alters their chicken colonization ability.

Previous studies within our lab group have clearly demonstrated that LuxS is critical for IA3902 pathogenesis, as the loss of LuxS led to significantly reduced *in vivo* colonization in both chickens and guinea pigs (10). The fact that the loss of LuxS does not lead to a similar loss of the ability to colonize chickens in the genetically similar but nonabortive strain NCTC 11168 (W7) made this topic an intriguing area of interest for further study, particularly as previous additional studies within our lab have failed to identify an explanation for this difference (10, 24, 25). Comparative genomics between NCTC 11168 (W7) and IA3902 revealed differential distribution of the *metAB* genes, putatively connected to the methionine biosynthesis cascade. The identification of a redundant methionine biosynthesis pathway in W7 but not in IA3902 provided a possible explanation for the colonization defect related to alterations in bacterial central metabolism. While there have been extensive studies regarding the contribution of LuxS to *C. jejuni* colonization, limited information exists about the contribution of L-met biosynthesis to *C. jejuni* colonization (10, 16). Thus, the study of central metabolism such as L-methionine biosynthesis represented an underexplored area for further investigation of the host-microbe relationship in *C. jejuni*.

Several critical prokaryotic cellular functions are dependent upon L-met availability, including (i) translation initiation, (ii) polypeptide biosynthesis, (iii) protein folding and secondary structure, and (iv) downstream utilization within the AMC (19, 26, 27). Disruption of L-met biosynthesis capabilities in pathogens such as *Staphylococcus aureus* and *Pseudomonas aeruginosa* has been shown to cause phenotypic defects in the ability to produce biofilms and lower growth rates *in vitro* (27). Thus, it has been surmised that translation rates and corresponding protein production are reduced during L-met metabolic constraint, resulting in an inability for cells to survive (26, 27). It is also highly likely that pathogenic microbes will encounter limiting L-met concentrations *in vivo* and will need to compete for this limited supply with either resident microflora or with the host itself, as L-met is required by both prokaryotes and vertebrates (19, 20, 26, 27). For example, human serum contains around 4 $\mu$g $\cdot$ ml$^{-1}$ L-met (28), and L-met is one of the least abundant amino acids available in human physiological fluids (27). Additionally, one of the first limiting amino acids in poultry diets is L-met, which strongly indicates that L-met availability in the chicken gut may frequently be limited (29). Disruption of the production or acquisition of L-met has been shown to result in reduced *in vivo* colonization ability in multiple pathogenic microbes, including *Mycobacterium tuberculosis* (26), *Streptococcus pneumoniae* (28), *Klebsiella pneumoniae* (30), *S. aureus* (31), and *Acinetobacter baumannii* (32). Thus, adequate availability of L-met appears to be critical to the survival and pathogenicity of many bacterial pathogens.

It is highly likely that *Campylobacter* will encounter limiting L-met concentrations *in vivo* and will need to compete for this limited supply with either resident microflora or the host itself. This would make the IA3902 Δ*luxS* strain, which lacks any known alternative L-met biosynthesis pathways, more susceptible to low L-met both intracellularly and extracellularly, compared to the W7 Δ*luxS* strain, which harbors the redundant MetAB system. As demonstrated in our study, introducing *metA* and *metB* into the genome of the IA3902 Δ*luxS* strain partially rescued the colonization defect in IA3902 Δ*luxS* at 5, 12, and 19 dpi (Fig. 6). Conversely, disruption of *metAB* in the W7 Δ*luxS* background significantly reduced colonization at 12 and 19 dpi. Taken together, our results demonstrate the critical importance for additional pathways of L-met production and/or transport after disruption of *luxS*, and they strongly suggest that L-met biosynthesis is critical for optimal *C. jejuni* colonization of chickens.

Interestingly, W7 Δ*luxS* Δ*metAB* mutants lacking *metA* and *metB* were still able to colonize chickens, albeit at a lower level. This is consistent with the finding that while L-met levels were decreased *in vitro* in the W7 Δ*luxS* Δ*metAB* mutant, they were not eliminated, nor were they eliminated in the IA3902 Δ*luxS* strain (Fig. 6). This strongly suggests that additional mechanisms for L-met production or uptake exist in *C. jejuni*. The biosynthetic production and transportation of L-met has been demonstrated to vary substantially among bacteria based on enzymes encoded on the genomes (20, 33, 34). In addition to biosynthesis capabilities, recent studies have identified the existence of methionine transporters in many bacteria that can influence cellular L-met levels through acquisition of L-met from the environment. In particular, the ABC transporter gene cluster MetNIQ has been identified to function to import L- and D-methionine in both *E. coli* and *Salmonella* (20, 33, 34). Husna et al. demonstrated in *Salmonella enterica* subsp. *enterica* serovar Typhimurium that *metNIQ* mutation was needed in conjunction with *metB* disruption to result in significant reduction of colonization in the spleen and liver in mice (20). Further analysis of *metNIQ* in *C. jejuni* via BLASTN search reveals a region on the genome of both IA3902 and W7 with partial homology to *E. coli metNIQ*, and a recent study has also identified these *metN* and *metQ* homologs to be important for *C. jejuni* mice colonization (35). Therefore, differences in methionine transport activity of *metNIQ in vivo*, or in that of other strain-specific methionine transporters, could explain the partial disruption of colonization observed in the W7 Δ*luxS* Δ*metAB* strain.

Indeed, both amino acid metabolism and transport have previously been demonstrated, utilizing *in vivo* animal models, to be essential for *C. jejuni* colonization (35, 36). For example, amino acid L-serine catabolism has been demonstrated to be critical for *C. jejuni* survival within the chicken cecum environment, as L-serine feeds directly into central metabolism (36). Gao et al. also demonstrated a total of 18 amino acid metabolism- and transport-related genes that were critical for normal *C. jejuni* strain 81-176 mouse colonization; in addition to the previously discussed methionine ABC transporter genes (*metQ* and *metN*), aspartate aminotransferase genes (*aspB* and *aspB-2*) and the aspartate binding transporter gene *peb1* were also found to be essential for colonization (35). Interestingly, aspartate is used for homoserine production, and homoserine is then utilized by *metAB* to produce homocysteine for conversion to L-met (37). Thus, these data also strongly suggest that the availability of amino acids such as methionine and aspartate for appropriate functioning of the AMC may be critical for normal *in vivo* colonization by *C. jejuni*. A previous study using the hard-agar plug method has also demonstrated that *C. jejuni* 81-176 *luxS* mutants have altered chemotactic response, as the mutant strain migrates toward the amino acids aspartate, asparagine, glutamate, and glutamine (38). Four amino acids, namely serine, proline, glutamate, and aspartate, have also been demonstrated to be essential for *C. jejuni* growth *in vitro* (39). Taken together, these studies indicate that certain amino acids are critical for *C. jejuni* survival, and many of these are metabolically disrupted by mutating *luxS* of *C. jejuni*. Further work using our mutant library to test AMC or AI-2 contributions to these amino acid metabolic disturbances is thus warranted.

In addition to disruption of methionine transport via *metN* and *metQ*, *S*-adenosylmethyltransferase (*mraW*), SAM synthase (*metK*), and a radical SAM domain-containing protein have also been shown to result in a significant mouse colonization defects when mutated in *C. jejuni* 81-176 (35). SAM, which is produced downstream of L-met within the AMC, has been demonstrated to be involved in a wide variety of cellular functions, including methylation of DNA, RNA, lipids, and proteins (40–42) and synthesis of polyamines and vitamins formed by SAM-dependent reactions (41). During our study, *in vitro* TR-FRET analysis revealed that the IA3902 Δ*luxS* and W7 Δ*luxS* strains had slight decreases (nonsignificant) in both L-met and SAM concentrations (Fig. 5). A decrease in L-met and SAM concentrations has also been observed in IA3902 Δ*luxS* in a previous study in our lab utilizing LC-electrospray ionization (ESI)-MS/MS (24). In that study, the IA3902 Δ*luxS* strain was demonstrated to have reduced homocysteine levels, as well as increased *S*-ribosylhomocysteine levels (24). In the current study, the IA3902

Δ*luxS*::*metAB* and W7 Δ*luxS* Δ*metAB* mutants demonstrated significant metabolic changes to L-met and SAM concentrations using the *in vitro* TR-FRET assays, which confirmed that genes *metAB* are directly connected to L-met biosynthesis and downstream SAM production in *C. jejuni* (Fig. 5). As basal levels of each AMC metabolite required for *in vivo* colonization and strain-specific utilization of each AMC metabolite are currently unknown, further research into the role of SAM in *in vivo* colonization by *C. jejuni* is also warranted.

As only partial recovery or disruption of chicken colonization occurred when evaluating our newly generated mutants, this suggested that other factors besides L-met biosynthesis feeding into the AMC may play a role in the observed phenotypes. Our mutagenesis strategy intentionally did not enable metabolic recovery of all known byproducts of LuxS, specifically AI-2. Thus, partial colonization recovery or disruption indicates that AI-2 utilization may still play a role in altered colonization in *luxS* mutants. Within the chicken enteric microenvironment, other microbes such as *Enterobacteriaceae* and *Enterococcus* spp. can also produce AI-2, which may be able to influence other bacterial species through uptake from the environment (38). The ability of *Campylobacter* spp. to take up AI-2 is currently debatable, as they lack both currently known AI-2 uptake receptor systems, the two-component sensor kinase LuxPQ and the Lsr receptor complex (43, 44). Additionally, some studies have suggested that *C. jejuni* can internalize AI-2, while others were unable to demonstrate the same response (45, 46). The addition of AI-2 has also been demonstrated to functionally complement phenotypic deficiencies of *luxS* mutants depending upon the strain utilized (38, 47). *C. jejuni* does harbor several ABC transporter systems with unknown functions that could serve as AI-2 transporters (43, 44). Additionally, new research suggests that as-yet-unknown AI-2 transporters may serve as a regulatory feature of the small RNA CjNC110 in IA3902 (13). Furthermore, additional independent chicken colonization trials have also resulted in *C. jejuni luxS*-deficient mutants able to partially colonize chickens during early days postinoculation (38). In that study, Quinones et al. reported significantly decreased but not completely eliminated colonization of chickens using *C. jejuni* 81-176 *luxS*-deficient mutants after 4 dpi. Similar to W7, strain 81-176 also harbors the additional *metAB* genes for alternative L-met production (12). However, this phenotype is most similar to our IA3902 Δ*luxS*::*metAB* mutant, whereby colonization was still present but was significantly decreased compared to the wild type, rather than to the W7 Δ*luxS* strain, which demonstrates no alteration in colonization ability. This suggests that other genetic differences between strains beyond additional L-met production pathways may also play a role in the ability of *luxS* mutants to colonize normally, or that AI-2 uptake from the gut microbiome may affect colonization by *Campylobacter luxS*-deficient mutants. The AI-2 derivative specifically utilized by *C. jejuni* and the basal levels required for colonization for each strain are currently unknown. Taken together, further exploration into the direct role AI-2 plays and the strain-specific utilization of AI-2 is also warranted.

Partial recovery of colonization in the IA3902 Δ*luxS*::*metAB* strain could also be due to a negative feedback loop of SAM due to an influx of excessive L-met feeding into the AMC, as our mutant was determined to overproduce both AMC products compared to wild-type IA3902 *in vitro* (Fig. 7). In bacteria, SAM can be converted to 5′-methylthioadenosine (MTA) by spermidine synthase; MTA is a polyamine synthesis inhibitor that is known to influence DNA replication (41, 48, 49). Spermidine synthase polyamine production has previously been demonstrated to be essential for *in vitro* growth of *C. jejuni* (50). SAM can also be converted to 5′-deoxyadenosine (5′dADO) by radical SAM enzymes; 5′dADO is a potent inhibitor of DNA methyltransferases, and it sequesters vitamins, the availability of which is essential to central metabolism (41, 42, 51). Thus, an influx of excess SAM *in vivo* and the resulting increased metabolic pathway production of MTA and 5′dADO could indirectly be leading to growth inhibition *in vivo* where methylation events, cell growth, and DNA replication contribute to cell survival.

Additional genes and phenotypes have been associated with chicken colonization fitness in *Campylobacter*, and differences between strains in these key areas may offer

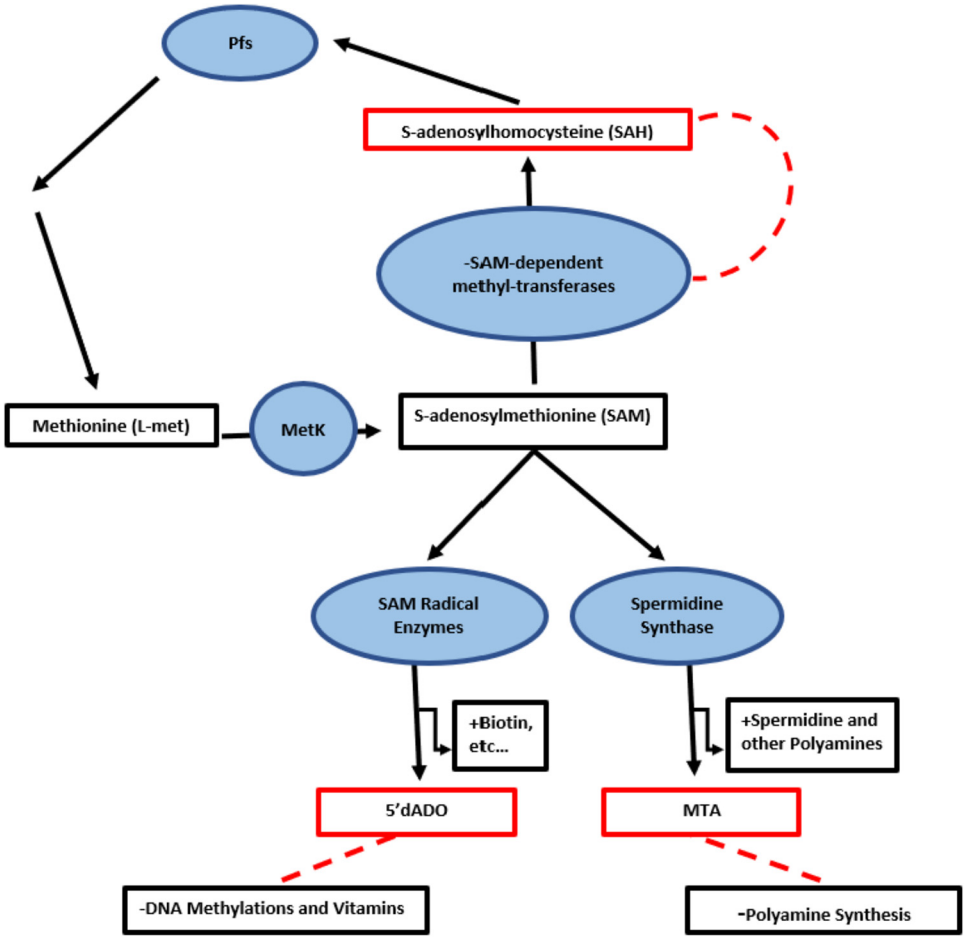


**FIG 7** Inhibitory metabolic products of the activated methyl cycle (AMC). Boxes indicate metabolic products of enzymes within or interconnected to the AMC cycle. Circles indicate the following enzymes: Pfs, *S*-adenosylhomocysteine nucleosidase; MetK, SAM synthase; SAM-dependent methyl transferases; SAM radical enzymes; and spermidine synthase. MetK produces SAM, which enables transfer of methyl groups ($-CH_3$) to various substances and is used by SAM-dependent reactions, namely SAM-dependent methyl transferases, SAM radical enzymes, and spermidine synthase. Red boxes indicate inhibitory AMC metabolic byproducts, namely SAH, *S*-adenosylhomocysteine; 5′dADO, 5′-deoxyadenosine; and MTA, 5′-methylthioadenosine. Red dashed lines indicate inhibitory interactions. SAH is toxic to the cells and must be recycled by Pfs.

an additional hypothesis for why introduction of MetAB was not enough to fully restore the colonization ability of the IA3902 Δ*luxS* strain. Other studies have demonstrated that flagella and flagellar motility are essential for chicken colonization (22, 23, 52, 53). For example, mutants lacking flagellins or regulators of flagellar biosynthesis, such as FlgR, $\sigma$54 (*rpoN*), and $\sigma$28 (*fliA*), have defects in chicken colonization (22, 53, 54). The *in vitro* motility assay demonstrated that IA3902 and W7 *luxS* mutants have disrupted motility, and recovery or disruption of L-met biosynthesis did not significantly alter motility levels, suggesting that the motility defect is independent of L-met availability (Fig. 4). Investigation of cell shape and flagellar morphology in *C. jejuni* strain 81116 using transmission electron microscopy comparing wild-type and *luxS* mutants found no significant differences between the strains (55). Additional work by our lab group in IA3902 and W7 has also demonstrated no differences in flagellar morphology of *luxS* mutants between strains (24). Previous studies have demonstrated that AI-2 complementation can restore motility defects of *C. jejuni luxS* mutants, suggesting that alteration in motility may be related to the loss of AI-2 due to *luxS* mutation instead of loss of L-met synthesis (38, 47). Increased concentrations of *S*-ribosylhomocysteine, as reported in *luxS* mutants in *C. jejuni* (24), has also been demonstrated to significantly increase biofilm formation in *Listeria monocytogenes*, promoting a sessile state as

**TABLE 3** Bacterial strains used in this study

| Species or strain | Description[a] | Source or reference |
|---|---|---|
| *Campylobacter jejuni* | | |
| W7 | Wild-type motile variant of NCTC 11168 | 10 |
| W7 Δ*luxS* | Δ*luxS*::Kan$^r$ | 10 |
| W7 Δ*luxS* Δ*metAB* | Δ*luxS*::Kan$^r$; Δ*metAB*::Apr$^r$ | This study |
| Sheep abortion clone IA3902 | Wild-type *C. jejuni* IA3902 | 58 |
| IA3902 Δ*luxS* | Δ*luxS*::Kan$^r$ | 10 |
| IA3902 Δ*luxS*::*metAB* | Δ*luxS*::Kan$^r$; ::*metAB*::Apr$^r$::Cm$^r$ | This study |
| *Escherichia coli* | | |
| DH5α | *fhuA2* Δ(*argF-lacZ*)U169 *phoA gln*V44 Φ80 Δ(*lacZ*)M15 *gyrA*96 *recA1 relA1 endA1 thi-1 hsdR*17 | NEB, Ipswich, MA |

[a]Resistance cassettes: Kan$^r$, kanamycin; Cm$^r$, chloramphenicol; Apr$^r$, apramycin.

opposed to a free-living planktonic state (56, 57). This again indicates other AMC byproducts, such as *S*-ribosylhomocysteine and AI-2, could be playing a role in colonization alterations in *luxS* mutants. As our study lacks characterization of a complete AMC metabolic profile of our mutant constructs, it is difficult to make definitive conclusions on potential metabolic disruption or recovery when comparing our mutants. To that end, further investigation using our mutant library in both limiting and standard MH media, followed by more complete metabolomic profiling, could reveal additional contributing metabolic factors and is thus warranted to continue to investigate differences between strains that account for altered colonization ability.

In summary, the dual function of the LuxS enzyme, which produces AI-2 and homocysteine for L-met biosynthesis, has previously complicated the ability to determine which metabolic byproduct(s) specifically contribute to phenotypic defects observed after disrupting *luxS* in various strains of *C. jejuni*. During this study, we demonstrated that the availability of additional pathways for L-met biosynthesis conferred by *metAB* is critical for colonization within the chicken cecum environment in *luxS*-deficient mutants, and we expanded knowledge on the contribution of the MetAB proteins to the intracellular L-met pool in *C. jejuni*. Production and acquisition of L-met provide intriguing therapeutic targets within the central metabolism of *C. jejuni*, as disruption appears to negatively impact cell growth and survival *in vivo*. It is still unclear what additional metabolic perturbances drive differences in *C. jejuni luxS*-deficient mutant phenotypic defects; however, the current study strongly supports the role of L-met biosynthesis as a critical component of the AMC important for *in vivo* colonization. Further exploration of methionine metabolism, AMC-interrelated pathways, and AI-2 utilization by *Campylobacter* remains warranted.

## MATERIALS AND METHODS

**Bacterial strains, plasmids, and culture conditions.** During this comparative study, two *C. jejuni* strains were used. *C. jejuni* IA3902 was utilized as the prototypical isolate of the sheep abortion (SA) clone (58). *C. jejuni* W7 is a highly motile variant of laboratory strain *C. jejuni* NCTC 11168, which is genetically similar to IA3902 but lacks the ability to induce abortion (9, 10, 12). *C. jejuni* strains and their isogenic mutants were routinely grown using Mueller-Hinton (MH) broth or agar plates (Becton, Dickinson, Franklin Lakes, NJ) at 42°C under microaerobic conditions (55% $O_2$, 10% $CO_2$, and 85% $N_2$) as previously described (13). For isogenic mutants containing a resistance cassette, the appropriate concentration of antibiotic was added to the medium (5 μg/ml chloramphenicol, 30 μg/ml kanamycin, or 15 μg/ml apramycin).

*Escherichia coli* DH5α competent cells (New England Biolabs, Ipswich, MA) containing plasmid constructs were grown at 37°C using Luria-Bertani (LB) agar plates or broth (Becton, Dickinson, Franklin Lakes, NJ) with shaking at 125 rpm. When appropriate, 50 μg/ml kanamycin, 20 μg/ml chloramphenicol, or 30 μg/ml apramycin was added to the broth or agar plates for selection of positive colonies.

All strains of *E. coli* and *C. jejuni* IA3902, W7, and respective isogenic mutants used in this study are listed in Table 3. All relevant constructed plasmids used for *C. jejuni* transformation are listed in Table 4. Relevant primer sequences are listed in Table 5. All strains were maintained in 20% glycerol stocks at −80°C and passaged from those stocks as needed for experimental procedures that followed.

**Basic local alignment searches and predictive operon search.** The Basic Local Alignment Search Tool (BLAST; https://blast.ncbi.nlm.nih.gov/Blast.cgi), was used to screen the genomes of both IA3902 (NCBI:txid567106) and W7 (reference genome NCTC 11168, NCBI:txid192222) for DNA and protein sequences related to L-met metabolism to identify similarities and differences between the strains.

**TABLE 4** Plasmids used

| Plasmid[a] | Description[b] | Source or reference |
|---|---|---|
| pUC19 | Commonly used cloning vector with Amp$^r$ | NEB, Ipswich, MA |
| pRRC | *Campylobacter* plasmid containing the *rrs-rrl* 16S/23S operon with Cm$^r$ | 59 |
| pUC19::Δ*metAB*::Apr$^R$ | pUC19 plasmid carrying *metAB* deletion via insertional deletion using Apr$^r$ | This study |
| pRRC::*metAB*::Apr$^r$ | pRRC plasmid carrying *metAB* insertion with Apr$^r$ selective marker | This study |

[a]pUC19 and pRRC are suicide plasmids.
[b]Resistance cassettes: Amp$^r$, ampicillin; Cm$^r$, chloramphenicol; Kan$^r$, kanamycin; Apr$^r$, apramycin.

*Escherichia coli* strain K-12 MG1655 (NCBI: taxid:511145) was screened against both IA3902 and W7 for methionine-related genes and proteins for comparison. The predictive operon algorithm web-based tool Operon-mapper (https://biocomputo.ibt.unam.mx/operon_mapper/) (21), was utilized to search the NCTC 11168 genes *metA* and *metB* located at nucleotide positions 1635432 to 1637686 (Cj1726c and Cj1727c) for operon structure.

**Creation of *C. jejuni* IA3902 Δ*luxS*::*metAB* and W7 Δ*luxS* Δ*metAB* mutants.** The IA3902 Δ*luxS*::*metAB* mutant was created via insertion of *metA* and *metB* into the intergenic region of the 16S and 23S rRNA operon (*rrs-rrl*) of the IA3902 Δ*luxS* strain (10) via homologous recombination using the backbone of plasmid pRRC (59), using synthetic double-stranded DNA fragments (Integrated DNA Technologies) and the Gibson assembly method (60). Briefly, the *metA* and *metB* genes, including approximately 250 bp upstream of the transcriptional start site, 250 base pairs downstream of the transcriptional stop site, and an apramycin antibiotic selective marker *aac(3)IV* (61) with a *cat* promoter, were cloned downstream of *metAB* into a XbaI-digested pRRC plasmid, to create pRRC::*metAB*. Next, using traditional cloning methods, pRRC::*metAB* was transformed into *E. coli* DH5α. Then, 5 μg of purified plasmid pRRC::*metAB* was used as a suicide vector for homologous recombination into the IA3902 Δ*luxS* strain introduced by electroporation (Bio-Rad) (62). For pure culture mutant selection, IA3902 Δ*luxS*::*metAB* cells were grown on MH agar containing chloramphenicol (5 μg/ml), kanamycin (30 μg/ml), and apramycin (15 μg/ml). The *metAB* gene insert and flanking region of the IA3902 rRNA operon (*rrs-rrl*) were amplified using forward and reverse primers pRRKconF1 and APRAR (Table 5). Following PCR amplification, product size was confirmed to be ~2,70 0bp, and Sanger sequencing was completed for confirmation of the correct gene sequence.

An isogenic mutant of the *C. jejuni* W7 Δ*luxS* mutant (10), the W7 Δ*luxS* Δ*metAB* mutant, was then created via insertional deletion mutagenesis again utilizing synthetic double-stranded DNA fragments (Integrated DNA Technologies) and the Gibson assembly method (60). The coding region of both *metA* and *metB* were replaced using the antibiotic selective marker apramycin *aac(3)IV* with a *cat* promoter (61), leaving approximately 250 bp upstream of transcriptional start site of *metB* and 250 bp downstream of the *metA* transcriptional stop site, knocking out the majority of coding sequence of both genes (Fig. 2). In brief, the gene fragment was cloned into a BamHI digested pUC19 plasmid (New England Biolabs, Ipswich, MA), to create pUC19::Δ*metAB*. Next, pUC19::Δ*metAB* was transformed into *E. coli* DH5α, and 5 μg of purified plasmid pUC19::Δ*metAB* was used as a suicide vector for homologous recombination into the W7 Δ*luxS* strain introduced by electroporation (Bio-Rad) (62). For pure culture mutant selection, W7 Δ*luxS* Δ*metAB* cells were grown on MH agar containing kanamycin (30 μg/ml) and apramycin (15 μg/ml). The *metAB* gene region with the insertional deletion knockout region and flanking regions were amplified using the forward and reverse primers METABconF1 and METABconR1 (Table 5). Following PCR amplification, product size was confirmed to be ~2,700 bp, and Sanger sequencing was completed for confirmation of the correct gene sequence.

**TABLE 5** Primer pairs used

| Target | Primer | Sequence | Source or reference |
|---|---|---|---|
| 16S-23S insertional region; ::*metAB* | pRRKconF1 | ATCGTAGATCAGCCATGCTA | This study |
| | METABconR1 | CAGGACTTGCTTCAGGTGTT | This study |
| 16S-23S insertional region; ::*apra*$^r$ | pRRKconF1 | ATCGTAGATCAGCCATGCTA | This study |
| | APRAR | ATTCTCGAGATAATCGACGC | This study |
| *metAB* chromosomal region | METABconF1 | TGCTTGGCACGCTTAATCTA | This study |
| | METABconR1 | CAGGACTTGCTTCAGGTGTT | This study |
| *metAB* chromosomal region for qRT-PCR | RTMETF | GGGTATATTTTCTGGAATAATCAGTGGCATTT | This study |
| | RTMETR | AAAATAGCGATGATTTGATAGCGGATTT | This study |
| 16S rRNA for qRT-PCR | 16SrRNA-F | TACCTGGGCTTGATATCCTA | 64 |
| | 16SrRNA-R | GGACTTAACCCAACATCTCA | 64 |
| *luxS* chromosomal region | 1198F4 | CAGCTCCTGCTGTGCGTTTAG | This study |
| | 1198R4 | TGGTTTGTTTGTGCCAAGTTAAGAAAG | This study |

All plasmids from *E. coli* DH5$\alpha$ were purified using the QIAquick plasmid miniprep kit (Hilden, Germany). All mutants were PCR amplified using high-fidelity TaKaRa *Ex Taq* DNA polymerase (TaKaRa Bio, USA), PCR products were purified using Qiagen QIAquick PCR purification kit (Hilden, Germany), and Sanger sequenced at the ISU DNA facility (Ames, IA) to validate mutant generation. All positive isogenic mutant colonies were screened for presence of motility as described below.

**Growth curves using IA3902 and W7 wild-type strains and respective isogenic mutants.** Growth curves were conducted in triplicate using IA3902 wild-type, IA3902 Δ*luxS*, IA3902 Δ*luxS*::*metAB*, W7-wild-type, W7 Δ*luxS*, and W7 Δ*luxS* Δ*metAB* strains (Table 3). The $A_{600}$ of overnight cultures was adjusted to 0.5 using sterile MH broth using a Genesys 10S VIS spectrophotometer (Thermo Scientific, USA). Cultures were diluted 1:10 for a final targeted starting $A_{600}$ of 0.05 in 125 ml of sterile MH broth and placed in a sterile 250-ml Erlenmeyer flask. Cultures were incubated at 42°C under microaerophilic conditions with shaking at 125 rpm for 30 h. Samples were removed from the flasks at designated time points (0, 4, 8, 12, 14, 24, 28, and 30 h). Samples were processed as described below for RNA isolation, protein isolation, and metabolite isolation, as well as for $A_{600}$ and colony counts using the drop plate method (63). Based on $A_{600}$ and preliminary CFU data (unpublished), W7 samples were processed at 14 h and IA3902 samples were processed at 12 h to ensure similar CFU counts for phenotypic comparisons, targeting the early stationary phase of growth. The average $A_{600}$ and CFU/ml over time were statistically analyzed using two-way ANOVA (GraphPad Prism). One-way ANOVA was used to analyze the collection time point (early stationary phase). A $P$ value of $<0.05$ was deemed significant.

**Motility assay using IA3902 and W7 wild-type strains and respective isogenic mutants.** Motility phenotype assays were conducted using the IA3902 wild-type, IA3902 Δ*luxS*, IA3902 Δ*luxS*::*metAB*, W7 wild-type, W7 Δ*luxS*, and W7 Δ*luxS* Δ*metAB* strains (Table 3). Motility was determined via inoculation of plates consisting of MH broth with 0.4% agar as previously described (13). The outermost zone of motility was measured at 30 h following incubation. All strains were evaluated for average motility using three biological replicates and six technical replicates per group. The three experiments were statistically analyzed using one-way ANOVA (GraphPad Prism), and differences between each strain were assessed via Tukey's multiple-comparison test. A $P$ value of $<0.05$ was deemed significant.

**Enumeration of *metA* and *metAB* transcriptional levels utilizing qRT-PCR.** To validate mutant *metAB* transcriptional expression levels, RNA was collected from the predetermined collection time point (early stationary phase). Analysis was conducted using strains with empirically determined nonsignificant ($P > 0.05$) optical density ($A_{600}$) and average CFU/ml. RNA was extracted from three separate biological replicates from IA3902 wild-type, W7 wild-type, IA3902 Δ*luxS*::*metAB*, and W7 Δ*luxS* Δ*metAB* strains. Briefly, 10 ml of cell culture was collected from each independent growth curve and spun to pellet cells at 8,000 $\times$ *g* for 2 min, and the supernatant was decanted. To extract RNA, cell pellets were mixed with 2 ml of QIAzol (Qiagen, Germantown, MD), pipetted up and down, vortexed at high speed for 1 min, and stored at room temperature for 15 min. QIAzol-extracted RNA from cultures was stored at −80°C before total RNA isolation using a Total MiRNeasy isolation kit (Qiagen, Germantown, MD) according to the manufacturer's instructions. On-column DNase treatment was performed using the RNase-free DNase set (Qiagen, Germantown, MD). Extracted RNA was then treated with the Turbo DNA-free kit (Life Technologies, Carlsbad, CA) to remove residual DNA contamination.

Extracted total RNA, converted to cDNA, was used to compare *metA* and *metB* mRNA and control 16S mRNA transcriptional levels utilizing quantitative reverse transcriptase PCR (qRT-PCR) as previously described (24, 64). Briefly, extracted RNA was converted to cDNA using an iScript cDNA synthesis kit (Bio-Rad, Hercules, CA) using 1,000 ng of total RNA. Samples were normalized to 100 ng cDNA using a Qubit BR DNA assay kit (Invitrogen, USA). Purity of cDNA was measured using the NanoDrop ND-1000 spectrophotometer prior to qRT-PCR analysis. qRT-PCR assays were performed using the SsoAdvanced universal SYBR green supermix kit (Bio-Rad, Hercules, CA) on the CFX Maestro real-time PCR detection system (Bio-Rad). Converted cDNA template for all samples were run in triplicate with reaction volumes of 15 $\mu$l. Amplification was conducted using 35 cycles of denaturation at 95°C for 10 s, as well as annealing for each primer pair set at 58°C for 30 s, using primers RTMETF and RTMETR or 16SrRNA-F and 16SrRNA-R (Table 5). The mRNA sequences of *metA* and *metB* were determined to be polycistronic, encoded as a single transcript, via Sanger sequencing at the Iowa State DNA Facility (Ames, IA) using PCR products from the qRT-PCR assay. Standard curves were generated for both mRNA 16S control and mRNA *metAB*, with efficiencies of $R^2 = 0.98$ and $R^2 = 0.99$, respectively. Relative fold change of transcription was calculated using the $2^{-\Delta\Delta CT}$ method and reported as the $\log_2$ fold change difference (65). The $C_T$ fold cutoff was set at 35, representing no detectible transcription. Statistical analyses were performed using one-way ANOVA (GraphPad Prism) followed by Tukey's multiple-comparison test to determine significance differences in gene expression levels between strains. A $P$ value of $<0.05$ was deemed significant.

**SDS-PAGE and liquid chromatography with tandem mass spectrometry proteomic analysis.** For extraction of whole cell protein, IA3902 Δ*luxS*::*metAB* and W7 Δ*luxS* Δ*metAB* bacterial cells were grown to the early stationary phase and collected. Briefly, MH broth cultures were harvested by taking 10 ml MH broth from two independent biological replicates and pelleted at 10,000 $\times$ *g* for 5 min at 4°C. The cell pellets were then resuspended in 5 ml of cold Dulbecco's phosphate-buffered saline (PBS) and spun again at 10,000 $\times$ *g* for 2 min at 4°C and decanted. This was repeated twice to wash the cell pellets. After the final spin, excess PBS was aspirated off the cell pellets. Next, 200 $\mu$l of lysis buffer (1$\times$ Tris-EDTA solution consisting of 1 Mm EDTA and 10 Mm Tris + 1% Triton X-100) was added to the protein pellets for resuspension. The resuspended cell pellets were then lysed mechanically using a Bullet Blender (NextAdvance, Troy, NY). To lyse the cells, 1.5-ml Eppendorf microcentrifuge tubes (Corning, Corning, USA) were loaded with sterilized 0.9- to 2.0-mm diameter stainless steel beads (NextAdvance, Troy, NY). The Bullet Blender was used for 5 min at maximum speed and stored at 4°C. Next, the lysed cells were

placed on ice for 15 min and vortexed for 1 min. Then, lysed cellular debris were spun at 10,000 × *g* at 4°C for 5 min. The supernatant was collected in a 1.5-ml microcentrifuge tube, and protein concentration was determined using the Qubit protein assay on the Qubit Fluorometer (Thermo Scientific). Similar protein extraction efficiency was validated prior to SDS-PAGE analysis. SDS-PAGE analysis was carried out by loading 15 μg of total protein into a Ready Gel precast 4 to 20% gradient SDS-PAGE gel (Bio-Rad) using extracted proteins of IA3902 wild-type, W7 wild-type, IA3902 Δ*luxS*::*metAB*, and W7 Δ*luxS* Δ*metAB* strains. Ten μl of Precision Plus Protein all blue standard (Bio-Rad) was loaded for protein molecular size determination. The electrophoresis was complete after 1 h and 30 min at 100 V. After electrophoresis, the SDS-PAGE gel was stained overnight with Coomassie brilliant blue (Thermo Scientific) and destained using 30% methanol (MeOH) with 1% acetic acid solution.

For protein alignment UniProt (https://www.uniprot.org/) was used to obtain protein sequences for MetA (34.2 kDa) and MetB (46.7 kDa) from reference strain *C. jejuni* NCTC 11168. Based on the predicted protein sizes, two gel slices were cut to extract MetA (34.2 kDa) and MetB (46.7 kDa) from the SDS-PAGE gel for each sample. Gel slices were placed in 100% methanol-pretreated 1.5-ml microcentrifuge tubes with 20 μl of 1% acetic acid solution. Next, gel slices were digested overnight in solution with trypsin/Lys-C using an Investigator ProGest automated digester (Genomic Solutions, Ann Arbor, USA). Following digestion, proteomic analysis was performed via liquid chromatography with tandem mass spectrometry (LC-MS/MS) using a Q Exactive hybrid quadrupole-Orbitrap mass spectrometer system (Thermo Fisher Scientific). The peptides were separated by liquid chromatography and analyzed by LC-MS/MS by fragmenting each peptide (66). The resulting fragmentation pattern was compared to a theoretical fragmentation pattern (67) to find peptides that could be used to identify proteins MetA and MetB.

For inclusion within the proteomic analysis, each biological replicate had threshold values of detection required, which included 2 unique peptide matches to protein MetA or MetB, 3 or more peptide spectrum matches (PSMs) with high confidence ($P < 0.001$), and an overall Mascot score, which takes the sum of scores of all PSMs detected (~95% confidence in protein detection). greater than 100. Individual PSMs with a retention time at or above 30 min were eliminated to remove wash step false positives. The averages of unique peptides, PSMs, and Mascot scores from each biological group were taken after threshold value filtering (Table 2). Data filtering was conducted using Proteome Discoverer 2.2 (Thermo Fisher Scientific).

**L-Methionine and SAM metabolite extraction and quantification.** Time-resolved fluorescence resonance energy transfer (TR-FRET) assays (Mediomics, LLC) were used to measure intracellular L-met and SAM concentrations, as previously described in other bacterial species such as *E. coli* and *Salmonella* spp. (68). During this assay, intracellular metabolites were extracted to quantify both L-met and SAM from three biological replicates at the collection time point (early stationary phase), according to the manufacturer's instructions with some modifications. Briefly, MH broth cultures were harvested from each respective growth curve as described above by taking 10 ml of MH broth from 250-ml Erlenmeyer flasks, then pelleted at 10,000 × *g* for 5 min at 4°C. The cell pellets were then resuspended in 5 ml of distilled water ($dH_2O$) and spun again at 10,000 × *g* at 4°C for 2 min and decanted. This was repeated twice to wash the cell pellets. After the final spin, excess $dH_2O$ was carefully aspirated off the cell pellets. CM buffer (Mediomics, LLC) was diluted to a 1:1 ratio using filter-sterilized $dH_2O$. Next, 200 μl of diluted CM buffer was added to 20 mg of cell pellet from each respective strain to lyse the cells to obtain intracellular metabolites. Cells were lysed by incubating the CM buffer and cell pellet slurry at room temperature for 60 min and vortexed occasionally. The lysate was then incubated on ice at 4°C for 15 min and then vortexed for 1 min. Next, the lysate was centrifuged at 12,000 × *g* for 5 min at 4°C. The supernatant was then transferred to 4°C prechilled 1.5-ml microcentrifuge tubes. The lysate was then snap-frozen using liquid nitrogen and stored at −80°C, for downstream L-met and SAM quantitative analysis. The supernatant containing metabolites was used for both L-met and SAM quantitative analysis.

For L-met quantitative analysis, the TR-FRET Bridge-It L-methionine fluorescence assay kit was used according to the manufacturer's instructions for bacterial cell cultures (Mediomics, LLC). All buffers and enzymes were preheated at 37°C for 30 min prior to assay setup. Briefly, 4 μl of supernatant was added to 6 μl of the mixture of enzyme solution L and buffer L (mastermix). The standard was prepared using the same mastermix for reproducibility of the assay. Next, 5 μl from each experimental sample and the standards were added to a 96-well plate (Mediomics, LLC) and incubated at 37°C for 20 min. Then, 45 μl of TR-FRET SAM assay solution was added to each well of the 96-well plate that contained experimental sample and standards, and each well was mixed by pipetting up and down 5 times. Two wells had 50 μl of $dH_2O$ added to act as a negative control. Next, the plate was covered and incubated at room temperature for 30 min according to the manufacturer's instructions.

For SAM quantitative analysis, the Bridge-It *S*-adenosyl methionine fluorescence assay kit was used according to the manufacturer's instructions for bacterial cell cultures (Mediomics, LLC). Briefly, the SAM assay solution was preheated at room temperature for 30 min prior to assay setup. Next, 10 μl of supernatant was added to the wells of a 96-well plate (Mediomics, LLC). The standard was prepared using the same mastermix for reproducibility of the assay. Then, 90 μl of SAM assay solution was added to each well of the 96-well plate that contained experimental sample and standard, and each well was mixed by pipetting up and down 5 times. Two wells had 100 μl of $dH_2O$ added acting as a negative control. Next, the plate was covered and incubated at room temperature for 30 min according to the manufacturer's instructions.

For both L-met and SAM quantitative analysis, experimental samples were run in duplicate using 3 biological replicates and the average fluorescence was calculated using the FLUOstar Omega microplate

reader (BMG Labtech, Ortenburg, Germany). To eliminate background, raw fluorescence (RF) was calculated using relative intensity of the 0 $\mu$M L-met standard ($F_0$) or 0 $\mu$M SAM standard ($F_0$) and fluorescence (F) of the experimental sample [(*F*): RF = $F - F_0$)]. L-Met or SAM levels were determined by using their respective standard curves and dilution factors; both $R^2$ values for the standard curves were above 0.96. For statistical analysis, one-way ANOVA (GraphPad Prism) with Tukey's multiple-comparison test was performed taking the average of the three biological replicates for each respective strain to determine significance between groups. A *P* value of $<0.05$ was deemed significant.

**Chicken colonization study and CFU enumeration.** All studies involving animals were approved by the Iowa State University Institutional Animal Care and Use Committee (IACUC) (protocol no. 1-18-8675-G) prior to initiation and followed all appropriate animal care guidelines. To investigate the effect of *metA* and *metB* on the ability of *Campylobacter* to colonize chickens, IA3902 wild-type, IA3902 Δ*luxS*, IA3902 Δ*luxS*::*metAB*, W7 wild-type, W7 Δ*luxS*, and W7 Δ*luxS* Δ*metAB* strains were used in a 3-week-long study as previously described (10, 13). For this study, 3-day-old commercial broiler chickens were randomly assigned to a treatment group with a minimum of 18 birds per group. Each biological group was housed in separate brooders. All birds were confirmed to be *Campylobacter* free via screening of cloacal swabs and plating on MH agar containing both selective supplement (SR0204E) and growth supplement (SR0232E) (Oxiod). Next, each bird group was orally inoculated via gavage with 200 $\mu$l bacterial suspension containing $\sim 5 \times 10^7$ CFU/ml of each respective strain. The weekly colonization levels in a minimum of 6 birds per groups were determined at necropsy performed at 5, 12, and 19 days postinoculation (dpi). Cecal contents were collected aseptically, and CFU (CFU) were determined following appropriate 10-fold serial dilutions for each bird. The serial dilution series were plated on the selective MH agar plates and incubated at 42°C under microaerobic conditions for up to 3 days. Representative isolates each week were plated onto selective medium containing the appropriate selective antibiotic marker for mutant detection for each respective group that had *Campylobacter* colonization. The limit of detection (LOD) was determined to be 100 CFU/g (i.e., a single colony present on the first dilution plate), while the range of accurate quantification was considered to be 30 to 300 CFU per plate (69). Whenever possible, plates were selected and counted based on the range of accurate quantification; however, if the only growth was present on the first dilution at less than 30 CFU, this actual CFU number was used for analysis. If no *Campylobacter* colonies were detected on the first dilution plate, the 100 CFU/g LOD was utilized for statistical analysis. For statistical analysis, significant difference in colonization ability ($P < 0.05$) was tested using one-way ANOVA (GraphPad Prism) with Tukey's multiple-comparison test to determine significant differences in colonization ($P < 0.05$) using the geometric mean between biological groups at each dpi point, using the null hypothesis that colonization levels between groups are the same at each dpi point. Bacterial lawns were also collected from each group for PCR analysis and used as confirmation of no cross-contamination between biological groups. To extract DNA, lawns were first resuspended in MH broth and then extracted using a Quick DNA miniprep kit (Zymo Research, Orange County, CA) to extract DNA according to the manufacturer's instructions. A total of 50 ng of DNA was inputted per PCR amplification reaction, and amplifications were carried out using high-fidelity *Ex Taq* DNA polymerase (TaKaRa Bio USA, USA). Primers used with specific gene targets are listed in Table 5.

## SUPPLEMENTAL MATERIAL

Supplemental material is available online only.

**SUPPLEMENTAL FILE 1**, PDF file, 0.5 MB.

## ACKNOWLEDGMENTS

We thank Lei Dai for assistance with mutant construction methodologies and Avanti Sinha for primer design technique.

## REFERENCES

1. Tang Y, Sahin O, Pavlovic N, LeJeune J, Carlson J, Wu Z, Dai L, Zhang Q. 2017. Rising fluoroquinolone resistance in *Campylobacter* isolated from feedlot cattle in the United States. Sci Rep 7:494. https://doi.org/10.1038/s41598-017-00584-z.
2. Gormley FJ, Little CL, Rawal N, Gillespie IA, Lebaigue S, Adak GK. 2011. A 17-year review of foodborne outbreaks: describing the continuing decline in England and Wales (1992–2008). Epidemiol Infect 139:688–699. https://doi.org/10.1017/S0950268810001858.
3. Skarp CPA, Hänninen M-L, Rautelin HIK. 2016. Campylobacteriosis: the role of poultry meat. Clin Microbiol Infect 22:103–109. https://doi.org/10.1016/j.cmi.2015.11.019.
4. Heuvelink AE, van Heerwaarden C, Zwartkruis-Nahuis A, Tilburg JJHC, Bos MH, Heilmann FGC, Hofhuis A, Hoekstra T, de Boer E. 2009. Two outbreaks of campylobacteriosis associated with the consumption of raw cows' milk. Int J Food Microbiol 134:70–74. https://doi.org/10.1016/j.ijfoodmicro.2008.12.026.
5. Clark CG, Price L, Ahmed R, Woodward DL, Melito PL, Rodgers FG, Jamieson F, Ciebin B, Li A, Ellis A. 2003. Characterization of waterborne outbreak–associated *Campylobacter jejuni*, Walkerton, Ontario. Emerg Infect Dis 9:1232–1241. https://doi.org/10.3201/eid0910.020584.
6. Kaakoush NO, Castaño-Rodríguez N, Mitchell HM, Man SM. 2015. Global epidemiology of *Campylobacter* infection. Clin Microbiol Rev 28:687–720. https://doi.org/10.1128/CMR.00006-15.
7. Sahin O, Fitzgerald C, Stroika S, Zhao S, Sippy RJ, Kwan P, Plummer PJ, Han J, Yaeger MJ, Zhang Q. 2012. Molecular evidence for zoonotic transmission of an emergent, highly pathogenic *Campylobacter jejuni* clone in the United States. J Clin Microbiol 50:680–687. https://doi.org/10.1128/JCM.06167-11.
8. Sahin O, Yaeger M, Wu Z, Zhang Q. 2017. *Campylobacter*-associated diseases in animals. Annu Rev Anim Biosci 5:21–42. https://doi.org/10.1146/annurev-animal-022516-022826.
9. Burrough ER, Sahin O, Plummer PJ, Zhang Q, Yaeger MJ. 2009. Pathogenicity of an emergent, ovine abortifacient *Campylobacter jejuni* clone orally inoculated into pregnant guinea pigs. Am J Vet Res 70:1269–1276. https://doi.org/10.2460/ajvr.70.10.1269.
10. Plummer P, Sahin O, Burrough E, Sippy R, Mou K, Rabenold J, Yaeger M,

Zhang Q. 2012. Critical role of LuxS in the virulence of *Campylobacter jejuni* in a guinea pig model of abortion. Infect Immun 80:585–593. https://doi.org/10.1128/IAI.05766-11.
11. Sahin O, Terhorst SA, Burrough ER, Shen Z, Wu Z, Dai L, Tang Y, Plummer PJ, Ji J, Yaeger MJ, Zhang Q. 2017. Key role of capsular polysaccharide in the induction of systemic infection and abortion by hypervirulent *Campylobacter jejuni*. Infect Immun 85:e00001-17. https://doi.org/10.1128/IAI.00001-17.
12. Wu Z, Sahin O, Shen Z, Liu P, Miller W, Zhang Q. 2013. Multi-omics approaches to deciphering a hypervirulent strain of *Campylobacter jejuni*. Genome Biol Evol 5:2217–2230. https://doi.org/10.1093/gbe/evt172.
13. Kreuder AJ, Ruddell B, Mou K, Hassall A, Zhang Q, Plummer PJ. 2020. Small noncoding RNA CjNC110 influences motility, autoagglutination, AI-2 localization, hydrogen peroxide sensitivity, and chicken colonization in *Campylobacter jejuni*. Infect Immun 88:e00245-20. https://doi.org/10.1128/IAI.00245-20.
14. Pereira CS, Thompson JA, Xavier KB. 2013. AI-2-mediated signalling in bacteria. FEMS Microbiol Rev 37:156–181. https://doi.org/10.1111/j.1574-6976.2012.00345.x.
15. Keersmaecker SCJD, Varszegi C, Boxel N. v, Habel LW, Metzger K, Daniels R, Marchal K, Vos DD, Vanderleyden J. 2005. Chemical synthesis of (*S*)-4,5-dihydroxy-2,3-pentanedione, a bacterial signal molecule precursor, and validation of its activity in *Salmonella* Typhimurium. J Biol Chem 280:19563–19568. https://doi.org/10.1074/jbc.M412660200.
16. Plummer PJ. 2012. LuxS and quorum-sensing in *Campylobacter*. Front Cell Infect Microbiol 2:22. https://doi.org/10.3389/fcimb.2012.00022.
17. Vendeville A, Winzer K, Heurlier K, Tang CM, Hardie KR. 2005. Making "sense" of metabolism: autoinducer-2, LuxS and pathogenic bacteria. Nat Rev Microbiol 3:383–396. https://doi.org/10.1038/nrmicro1146.
18. Gölz G, Adler L, Huehn S, Alter T. 2012. LuxS distribution and AI-2 activity of *Campylobacter* spp. J Appl Microbiol 112:571–578. https://doi.org/10.1111/j.1365-2672.2011.05221.x.
19. Ferla MP, Patrick WM. 2014. Bacterial methionine biosynthesis. Microbiology (Reading) 160:1571–1584. https://doi.org/10.1099/mic.0.077826-0.
20. Husna AU, Wang N, Cobbold SA, Newton HJ, Hocking DM, Wilksch JJ, Scott TA, Davies MR, Hinton JC, Tree JJ, Lithgow T, McConville MJ, Strugnell RA. 2018. Methionine biosynthesis and transport are functionally redundant for the growth and virulence of *Salmonella* Typhimurium. J Biol Chem 293:9506–9519. https://doi.org/10.1074/jbc.RA118.002592.
21. Taboada B, Estrada K, Ciria R, Merino E. 2018. Operon-mapper: a web server for precise operon identification in bacterial and archaeal genomes. Bioinformatics 34:4118–4120. https://doi.org/10.1093/bioinformatics/bty496.
22. Hendrixson DR, DiRita VJ. 2004. Identification of *Campylobacter jejuni* genes involved in commensal colonization of the chick gastrointestinal tract. Mol Microbiol 52:471–484. https://doi.org/10.1111/j.1365-2958.2004.03988.x.
23. Bolton DJ. 2015. *Campylobacter* virulence and survival factors. Food Microbiol 48:99–108. https://doi.org/10.1016/j.fm.2014.11.017.
24. Mou KT, Plummer PJ. 2016. The impact of the LuxS mutation on phenotypic expression of factors critical for *Campylobacter jejuni* colonization. Vet Microbiol 192:43–51. https://doi.org/10.1016/j.vetmic.2016.06.011.
25. Mou KT, Muppirala UK, Severin AJ, Clark TA, Boitano M, Plummer PJ. 2014. A comparative analysis of methylome profiles of *Campylobacter jejuni* sheep abortion isolate and gastroenteric strains using PacBio data. Front Microbiol 5:782. https://doi.org/10.3389/fmicb.2014.00782.
26. Berney M, Berney-Meyer L, Wong K-W, Chen B, Chen M, Kim J, Wang J, Harris D, Parkhill J, Chan J, Wang F, Jacobs WR. 2015. Essential roles of methionine and *S*-adenosylmethionine in the autarkic lifestyle of *Mycobacterium tuberculosis*. Proc Natl Acad Sci U S A 112:10008–10013. https://doi.org/10.1073/pnas.1513033112.
27. Jochim A, Shi T, Belikova D, Schwarz S, Peschel A, Heilbronner S. 2019. Methionine limitation impairs pathogen expansion and biofilm formation capacity. Appl Environ Microbiol 85:e00177-19.
28. Basavanna S, Chimalapati S, Maqbool A, Rubbo B, Yuste J, Wilson RJ, Hosie A, Ogunniyi AD, Paton JC, Thomas G, Brown JS. 2013. The effects of methionine acquisition and synthesis on *Streptococcus pneumoniae* growth and virulence. PLoS One 8:e49638. https://doi.org/10.1371/journal.pone.0049638.
29. Zhang S, Gilbert ER, Noonan KJT, Saremi B, Wong EA. 2018. Gene expression and activity of methionine converting enzymes in broiler chickens fed methionine isomers or precursors. Poult Sci 97:2053–2063. https://doi.org/10.3382/ps/pey037.
30. Bachman MA, Breen P, Deornellas V, Mu Q, Zhao L, Wu W, Cavalcoli JD, Mobley HLT. 2015. Genome-wide identification of *Klebsiella pneumoniae* fitness genes during lung infection. mBio 6:e00775. https://doi.org/10.1128/mBio.00775-15.
31. Krismer B, Liebeke M, Janek D, Nega M, Rautenberg M, Hornig G, Unger C, Weidenmaier C, Lalk M, Peschel A. 2014. Nutrient limitation governs *Staphylococcus aureus* metabolism and niche adaptation in the human nose. PLoS Pathog 10:e1003862. https://doi.org/10.1371/journal.ppat.1003862.
32. Wang N, Ozer EA, Mandel MJ, Hauser AR. 2014. Genome-wide identification of *Acinetobacter baumannii* genes necessary for persistence in the lung. mBio 5:e01163-14–e01114. https://doi.org/10.1128/mBio.01163-14.
33. Merlin C, Gardiner G, Durand S, Masters M. 2002. The *Escherichia* coli *metD* locus encodes an ABC transporter which includes Abc (MetN), YaeE (MetI), and YaeC (MetQ). J Bacteriol 184:5513–5517. https://doi.org/10.1128/jb.184.19.5513-5517.2002.
34. Zhang Z, Feige JN, Chang AB, Anderson IJ, Brodianski VM, Vitreschak AG, Gelfand MS, Saier MH. 2003. A transporter of *Escherichia coli* specific for L- and D-methionine is the prototype for a new family within the ABC superfamily. Arch Microbiol 180:88–100. https://doi.org/10.1007/s00203-003-0561-4.
35. Gao B, Vorwerk H, Huber C, Lara-Tejero M, Mohr J, Goodman AL, Eisenreich W, Galán JE, Hofreuter D. 2017. Metabolic and fitness determinants for *in vitro* growth and intestinal colonization of the bacterial pathogen *Campylobacter jejuni*. PLoS Biol 15:e2001390. https://doi.org/10.1371/journal.pbio.2001390.
36. Velayudhan J, Jones MA, Barrow PA, Kelly DJ. 2004. L-Serine catabolism via an oxygen-labile L-serine dehydratase is essential for colonization of the avian gut by *Campylobacter jejuni*. Infect Immun 72:260–268. https://doi.org/10.1128/iai.72.1.260-268.2004.
37. Hofreuter D. 2014. Defining the metabolic requirements for the growth and colonization capacity of *Campylobacter jejuni*. Front Cell Infect Microbiol 4:137. https://doi.org/10.3389/fcimb.2014.00137.
38. Quiñones B, Miller WG, Bates AH, Mandrell RE. 2009. Autoinducer-2 production in *Campylobacter jejuni* contributes to chicken colonization. Appl Environ Microbiol 75:281–285. https://doi.org/10.1128/AEM.01803-08.
39. Guccione E, Leon-Kempis M. d R, Pearson BM, Hitchin E, Mulholland F, Diemen P. v, Stevens MP, Kelly DJ. 2008. Amino acid-dependent growth of *Campylobacter jejuni*: key roles for aspartase (AspA) under microaerobic and oxygen-limited conditions and identification of AspB (Cj0762), essential for growth on glutamate. Mol Microbiol 69:77–93. https://doi.org/10.1111/j.1365-2958.2008.06263.x.
40. Fontecave M, Atta M, Mulliez E. 2004. *S*-adenosylmethionine: nothing goes to waste. Trends Biochem Sci 29:243–249. https://doi.org/10.1016/j.tibs.2004.03.007.
41. Parveen N, Cornell KA. 2011. Methylthioadenosine/*S*-adenosylhomocysteine nucleosidase, a critical enzyme for bacterial metabolism. Mol Microbiol 79:7–20. https://doi.org/10.1111/j.1365-2958.2010.07455.x.
42. Challand M, Ziegert T, Douglas P, Wood R, Kriek M, Shaw N, Roach P. 2009. Product inhibition in the radical *S*-adenosylmethionine family. FEBS Lett 583:1358–1362. https://doi.org/10.1016/j.febslet.2009.03.044.
43. Cloak OM, Solow BT, Briggs CE, Chen C-Y, Fratamico PM. 2002. Quorum sensing and production of autoinducer-2 in *Campylobacter* spp., *Escherichia coli* O157:H7, and *Salmonella enterica* serovar Typhimurium in foods. Appl Environ Microbiol 68:4666–4671. https://doi.org/10.1128/aem.68.9.4666-4671.2002.
44. Rezzonico F, Duffy B. 2008. Lack of genomic evidence of AI-2 receptors suggests a non-quorum sensing role for *luxS* in most bacteria. BMC Microbiol 8:154. https://doi.org/10.1186/1471-2180-8-154.
45. Holmes K, Tavender TJ, Winzer K, Wells JM, Hardie KR. 2009. AI-2 does not function as a quorum sensing molecule in *Campylobacter jejuni* during exponential growth *in vitro*. BMC Microbiol 9:214. https://doi.org/10.1186/1471-2180-9-214.
46. Adler L, Alter T, Sharbati S, Gölz G. 2015. The signaling molecule autoinducer-2 is not internalised in *Campylobacter jejuni*. Berliner Und Münchener Tierärztliche Wochenschrift 128:111–116.
47. Adler L, Alter T, Sharbati S, Gölz G. 2014. Phenotypes of *Campylobacter jejuni luxS* mutants are depending on strain background, kind of mutation and experimental conditions. PLoS One 9:e104399. https://doi.org/10.1371/journal.pone.0104399.
48. Sekowska A, Dénervaud V, Ashida H, Michoud K, Haas D, Yokota A, Danchin A. 2004. Bacterial variations on the methionine salvage pathway. BMC Microbiol 4:9. https://doi.org/10.1186/1471-2180-4-9.
49. Sekowska A, Ashida H, Danchin A. 2019. Revisiting the methionine

salvage pathway and its paralogues. Microb Biotechnol 12:77–97. https://doi.org/10.1111/1751-7915.13324.
50. Hanfrey CC, Pearson BM, Hazeldine S, Lee J, Gaskin DJ, Woster PM, Phillips MA, Michael AJ. 2011. Alternative spermidine biosynthetic route is critical for growth of *Campylobacter jejuni* and is the dominant polyamine pathway in human gut microbiota. J Biol Chem 286:43301–43312. https://doi.org/10.1074/jbc.M111.307835.
51. North JA, Wildenthal JA, Erb TJ, Evans BS, Byerly KM, Gerlt JA, Tabita FR. 2020. A bifunctional salvage pathway for two distinct *S*-adenosylmethionine by-products that is widespread in bacteria, including pathogenic *Escherichia coli*. Mol Microbiol 113:923–937. https://doi.org/10.1111/mmi.14459.
52. Wassenaar TM, van der Zeijst BAM, Ayling R, Newell DG. 1993. Colonization of chicks by motility mutants of *Campylobacter jejuni* demonstrates the importance of flagellin A expression. J Gen Microbiol 139:1171–1175. https://doi.org/10.1099/00221287-139-6-1171.
53. Hendrixson DR. 2006. A phase-variable mechanism controlling the *Campylobacter jejuni* FlgR response regulator influences commensalism. Mol Microbiol 61:1646–1659. https://doi.org/10.1111/j.1365-2958.2006.05336.x.
54. Wassenaar TM, Fry BN, van der Zeijst BAM. 1993. Genetic manipulation of *Campylobacter*: evaluation of natural transformation and electrotransformation.Gene132:131–135.https://doi.org/10.1016/0378-1119(93)90525-8.
55. Jeon B, Itoh K, Misawa N, Ryu S. 2003. Effects of quorum sensing on *flaA* transcription and autoagglutination in *Campylobacter jejuni*. Microbiol Immunol 47:833–839. https://doi.org/10.1111/j.1348-0421.2003.tb03449.x.
56. Belval SC, Gal L, Margiewes S, Garmyn D, Piveteau P, Guzzo J. 2006. Assessment of the roles of LuxS, *S*-ribosyl homocysteine, and autoinducer 2 in cell attachment during biofilm formation by *Listeria monocytogenes* EGD-e. Appl Environ Microbiol 72:2644–2650. https://doi.org/10.1128/AEM.72.4.2644-2650.2006.
57. Hardie KR, Heurlier K. 2008. Establishing bacterial communities by "word of mouth": LuxS and autoinducer 2 in biofilm development. Nat Rev Microbiol 6:635–643. https://doi.org/10.1038/nrmicro1916.
58. Sahin O, Plummer PJ, Jordan DM, Sulaj K, Pereira S, Robbe-Austerman S, Wang L, Yaeger MJ, Hoffman LJ, Zhang Q. 2008. Emergence of a tetracycline-resistant *Campylobacter jejuni* clone associated with outbreaks of ovine abortion in the United States. J Clin Microbiol 46:1663–1671. https://doi.org/10.1128/JCM.00031-08.
59. Muraoka WT, Zhang Q. 2011. Phenotypic and genotypic evidence for L-fucose utilization by *Campylobacter jejuni*. J Bacteriol 193:1065–1075. https://doi.org/10.1128/JB.01252-10.
60. Gibson DG, Young L, Chuang R-Y, Venter JC, Hutchison CA, Smith HO. 2009. Enzymatic assembly of DNA molecules up to several hundred kilobases. Nat Methods 6:343–345. https://doi.org/10.1038/nmeth.1318.
61. Cameron A, Gaynor EC. 2014. Hygromycin B and apramycin antibiotic resistance cassettes for use in *Campylobacter jejuni*. PLoS One 9:e95084. https://doi.org/10.1371/journal.pone.0095084.
62. Davis L, Young K, DiRita V. 2008. Genetic manipulation of *Campylobacter jejuni*. Curr Protoc Microbiol 8:8A.2.1–8A.2.17.
63. Chen C-Y, Nace GW, Irwin PL. 2003. A 6×6 drop plate method for simultaneous colony counting and MPN enumeration of *Campylobacter jejuni*, *Listeria monocytogenes*, and *Escherichia coli*. J Microbiol Methods 55:475–479. https://doi.org/10.1016/S0167-7012(03)00194-5.
64. Han J, Sahin O, Barton Y-W, Zhang Q. 2008. Key role of Mfd in the development of fluoroquinolone resistance in *Campylobacter jejuni*. PLoS Pathog 4:e1000083. https://doi.org/10.1371/journal.ppat.1000083.
65. Livak KJ, Schmittgen TD. 2001. Analysis of relative gene expression data using real-time quantitative PCR and the $2^{-\Delta\Delta CT}$ method. Methods 25:402–408. https://doi.org/10.1006/meth.2001.1262.
66. Cox J, Mann M. 2011. Quantitative, high-resolution proteomics for data-driven systems biology. Annu Rev Biochem 80:273–299. https://doi.org/10.1146/annurev-biochem-061308-093216.
67. Koenig T, Menze BH, Kirchner M, Monigatti F, Parker KC, Patterson T, Steen JJ, Hamprecht FA, Steen H. 2008. Robust prediction of the MASCOT score for an improved quality assessment in mass spectrometric proteomics. J Proteome Res 7:3708–3717. https://doi.org/10.1021/pr700859x.
68. Heyduk E, Heyduk T. 2010. Fluorescent homogeneous immunosensors for detecting pathogenic bacteria. Anal Biochem 396:298–303. https://doi.org/10.1016/j.ab.2009.09.039.
69. Breed R, and, Dotterrer WD. 1916. The number of colonies allowable on satisfactory agar plates. J Bacteriol 1:321–331. https://doi.org/10.1128/JB.1.3.321-331.1916.